WISCONSIN HIGHWAY RESEARCH PROGRAM #0092-45-15

EFFECTIVENESS OF GEOSYNTHETICS IN STABILIZING SOFT SUBGRADES

FINAL REPORT

By

Steve Maxwell, Woon-Hyung Kim, Tuncer B. Edil,
and Craig H. Benson

Geotechnical Engineering Program
Department of Civil & Environmental Engineering
University of Wisconsin-Madison

SUBMITTED TO THE WISCONSIN DEPARTMENT OF TRANSPORTATION

October 31, 2005

ACKNOWLEDGEMENT

Financial support for the study described in this paper was provided by the Wisconsin Department of Transportation (WisDOT). Appreciation is expressed to Tensar Earth Technologies Inc., Ten Cate Mirafi, and Huesker Inc. for supplying the geosynthetics. The support of these parties is gratefully acknowledged. The findings and opinions expressed in this report are solely those of the authors and do not reflect the opinions or policies of WisDOT.

DISCLAIMER

This research was funded through the Wisconsin Highway Research Program by the Wisconsin Department of Transportation and the Federal Highway Administration under Project # 0092-45-15. The contents of this report reflect the views of the authors who are responsible for the facts and accuracy of the data resented herein. The contents do no necessarily reflect the official views of the Wisconsin Department of Transportation or the Federal Highway Administration at the time of publication.

Technical Report Documentation Page

1. Report No. 0092-45-15	2. Government Accession No	3. Recipient's Catalog No
4. Title and Subtitle Geosynthetics in Stabilizing Soft Subgrade with Breaker Run		5. Report Date (Print date) 6. Performing Organization Code
7. Authors Steve Maxwell, Woon-Hyung Kim, Tuncer B. Edil, and Craig H. Benson		8. Performing Organization Report No. 04-02
9. Performing Organization Name and Address Department of Civil and Environmental Engineering University of Wisconsin-Madison 1415 Engineering Drive Madison, WI 53706		10. Work Unit No. (TRAIS) 11. Contract or Grant No.
12. Sponsoring Agency Name and Address Wisconsin Department of Transportation 4802 Sheboygan Avenue Madison, WI 73707-7965		13. Type of Report and Period Covered Final Report, (Dates) 14. Sponsoring Agency Code

15. Supplementary Notes

16. Abstract

This report introduced the research begun in 1999 at the University of Wisconsin-Madison to further understand aspects of geosynthetic-reinforced subbases in a pavement system. To learn more about how the performance of highway pavement is improved with geosynthetics, a field demonstration was conducted using a 21-m section along a Wisconsin highway (USH 45) near Antigo, Wisconsin, that incorporated three test sub-sections. Three different geosynthetics including a woven geotextile and two different types of geogrids were evaluated for stabilization. The same pavement structure was used for all test sections except for the geosynthetics. Observations made during and after construction indicate that all sections provided adequate support for the construction equipment and that no distress is evident in any part of the highway. Much has been learned about instrumentation of geosynthetics with foil-type strain gages. The installation procedures and weatherization techniques used during this demonstration project appeared to be a success. Additionally, better strain gage results are possible for a geotextile when a longer (25 mm) strain gage is used. The falling weight deflectometer did not provide sufficient resolution to differentiate between different types of geosynthetic test sections especially in a field environment where there's heterogeneity of natural soils. However, a greater seasonal variability of the subgrade was noted. A control section without reinforcement was not constructed at this time that would have allowed for comparison and assessment of the geosynthetic addition.

17. Key Words Soft subgrade, geosynthetics, stabilization, pavement	18. Distribution Statement No restriction. This document is available to the public through the National Technical Information Service 5285 Port Royal Road Springfield VA 22161		
19. Security Classif.(of this report) Unclassified	19. Security Classif. (of this page) Unclassified	20. No. of Pages (pages)	21. Price

Form DOT F 1700.7 (8-72) Reproduction of completed page authorized

EXECUTIVE SUMMARY

A field demonstration was conducted using a 21-m section along a Wisconsin highway (USH 45) near Antigo, Wisconsin, that incorporated three test sub-sections. Three different geosynthetics including a woven geotextile and two different types of geogrids were evaluated for stabilization. The same pavement structure was used for all test sections except for the geosynthetics. Observations made during and after construction indicate that all sections provided adequate support for the construction equipment and that no distress is evident in any part of the highway.

Much has been learned about instrumentation of geosynthetics with foil-type strain gages. The falling weight deflectometer did not provide sufficient resolution to differentiate between different types of geosynthetic test sections. However, a greater seasonal variability of the subgrade was noted. A control section without reinforcement was not constructed at this time that would have allowed for comparison and assessment of the geosynthetic addition.

An additional investigation was conducted at STH 60 to delineate the effectiveness of geosynthetic reinforcement. According to this additional investigation, working platforms reinforced by geosynthetics accumulated deformation at a slower rate than unreinforced working platforms. As a result, total deflections were always smaller (about a factor of two) for reinforced working platforms relative to unreinforced working platforms. Smaller deflections were also associated with working platforms that were thicker or reinforced with less extensible geosynthetics.

TABLE OF CONTENTS

ACKNOWLEDGEMENTS …….. i

DISCLAIMER……. i

TECHNICAL REPORT DOCUMENTATION PAGE……...ii

EXECUTIVE SUMMARY……. iii

TABLE OF CONTENTS ……..… iv

TABLE OF TABLES ……..… vi

TABLE OF FIGURES ……..…….. vii

1. INTRODUCTION …….. 1

2. BACKGROUND ……..…… 5

2.1 Geosynthetic Types ……..… 5

2.2 Environmental Issues ……. 7

2.3 Highway Applications ……. 8

2.3.1 Unpaved Road …… 8

2.3.2 Paved Road ……..… 9

2.4 Geosynthetic Theories and Issues …… 11

2.4.1 Separation ……...11

2.4.2 Lateral Restraint ……12

2.4.3 Tensioned Membrane ……13

2.4.4 Modulus at Low Strain …….. 14

2.5 Design Methodologies ……..…… …. 15

2.5.1 “Barenburg” Method ……... 16

2.5.2 “Giroud” Method …….. 18

3. FIELD METHODS AND MATERIALS ……. 19

3.1 Application and Mechanisms ……... …..19

3.2 Geosynthetic Selection ……19

3.3 Strain Gage Selection ……..……..…20

3.4 Strain Gage Attachment ……21

3.5 Weatherization ……22

3.6 Test Section Orientation ……22

3.7 Data Collection ……27

3.8 Temperature Correction of Gage Measurements ……28

3.9 Strain Gage Calibration ……28

3.10 Falling Weight Deflectometer Test ……..31

3.11 Modulus Back-calculation ……37

4. RESULTS …..……41

4.1 Strain Gage Observations and Results ..……41

4.2 FWD Results ……..….43

5. ADDITIONAL INVESTIGATIONS ……..……..48

6. CONCLUSIONS AND RECOMMENDATIONS ……..……..50

REFERENCES ……53

TABLE OF TABLES

TABLE 1. Geosynthetic Properties ……..…….. 6

TABLE 2. Strain Data Summary ……..…….. 42

TABLE OF FIGURES

FIGURE 1. Picture of Geosynthetics: PGG, KGG, and WGT From Right to Left 7

FIGURE 2. Separation Theory: separated (unmixed), left and mixed, right .. 12

FIGURE 3. Lateral Restraint Function Showing Four Mechanisms of Improvement 13

FIGURE 4. Tensioned Membrane Function Showing Displacement and Resultant Force 14

FIGURE 5. PGG Section Showing Strain Gage Location and Orientation ... 24

FIGURE 6. KGG Section Showing Strain Gage Location and Orientation ... 25

FIGURE 7. WGT Section Showing Strain Gage Location and Orientation ... 26

FIGURE 8. Schematic of Electrical Circuit Showing Connections that Cancel Bending Strain 27

FIGURE 9. Calibration and Correlation for Geogrids 32

FIGURE 10. Calibration and Correlation for Geotextile 33

FIGURE 11. Right-hand Side View With Respect To Front of the FWD Showing LVDTs and Load Frame 34

FIGURE 12. Left Side View With Respect To Front of the FWD Showing LVDTs and Segmented Plate 35

FIGURE 13. Unconfined Compressive Strength, Antigo Silt Loam 40

FIGURE 14. Maximum Deflection From Falling Weight Deflectometer Tests After Construction, Winter, and Following Spring 44

FIGURE 15. Seasonal Deflection Basins Showing Greater Deflection in the Spring 45

FIGURE 16. Back-calculated Modulus at 40 kN for Each Layer along USH 45 Test Sections 47

1. INTRODUCTION

Geosynthetics are man-made plastics shaped in many forms (i.e. grids, textiles, nets and cells) that possess and may contribute significant tensile strength to the bottom portion of a highway pavement section. Although geosynthetics have many applications, the focus of this report is on quantitative observations to learn more about how highways are improved with geosynthetic. Geosynthetics are important for highway construction, since observations indicate better performance (i.e., less rutting associated with increased numbers of load repetitions) for highways constructed with geosynthetic-reinforced subbases. A geosynthetic-reinforced subbase is typically constructed above relatively soft subgrades and allows for thinner layers of base and surface courses above. The traditional and typically more costly alternative method for highway construction consists of replacing soft subgrades with thick granular and/or base course layers to insure support of the pavement surface.

Recent explorations indicate our predecessors strengthened walls and roads with natural materials (i.e., trees, branches, and other plant fibers). For example, the Great Wall of China utilized interbedded tree branches to reinforce successive layers of earthen material. Another historic example, a corduroy road provided a strong, improved road by laying logs together transversely to cross low-lying, swampy ground. More recently, a progression from natural materials to even stronger, more durable, man-made materials (geosynthetics) has happened. During the 1970's geosynthetics were available worldwide.

Currently, the numerous geosynthetic applications are understood to different degrees. Each application has numerous different physical mechanisms at work, which must be thoroughly understood to enable an engineer to design with geosynthetics. An understanding and effective design methodology exists for the geosynthetic application of reinforced retaining walls that are often constructed for steep embankment slopes. Such stronger, improved, geosynthetic-reinforced retaining walls constructed near Kobe, Japan, clearly demonstrated benefits by withstanding the 6.9 Magnitude earthquake that occurred on January 16, 1995. Thus, the problem regarding the highway application is a lack of understanding of the fundamental behavior of a geosynthetic-reinforced subbase. Presently, researchers continue to investigate and define mechanisms of how geosynthetics improve highways.

This report introduces the research begun in 1999 at the University of Wisconsin-Madison to further understand aspects of geosynthetic-reinforced subbases. This process began with a review of pertinent literature on the subject. A lack of consensus appears to exist in regards to the predominant mechanisms that affect the behavior and performance of pavements underlain by a geosynthetic-reinforced subbase. In an effort to further local knowledge, a field demonstration was initiated along State Highway 45 near Antigo, Wisconsin. The objectives of this effort included:

(1) successful installation of strain gages on three different types of geosynthetics,

(2) evaluation and refinement of strain gage installation, weatherization and data collection procedures,

(3) comparison of strain gage results and falling weight deflectometer results, and

(4) evaluation of the performance of geosynthetics-reinforced subbase layer.

Another objective achieved was to gain a better understanding of the behavior of an actual reinforced subbase below a highway pavement. Results consist of identification of successful instrumentation methods that allow for the direct measurement of tensile strain within a geosynthetic, which is part of a reinforced subbase. Additional results include confirmation of successful weatherization techniques and observation of highway performance utilizing falling weight deflectometer results. However, based on results, most conclusions are the basis for future recommendations and improvements allowing for successful collection of more data.

Understanding the basic physical mechanisms of how a geosynthetic reinforces a highway subbase as well as identifying and determining appropriate design methodologies are the overall goals of the on-going research at UW-Madison. Currently, several physical mechanisms, design methodologies and qualitative benefits have been defined. Realization of quantitative benefits of a geosynthetic-reinforced subbase is the ultimate goal of the on-going research at UW-Madison. With such knowledge tremendous savings are possible as a result of cheaper highway construction and reconstruction costs as well as longer pavement life cycles. These potentially large savings are what drives research to

further explore and clearly define the highway application of geosynthetics. Other benefits, such as safer, more comfortable highways, should not be overlooked but also contemplated as being simultaneously achieved when geosynthetics are utilized in routine highway construction.

More specifically, prior research and actual use have partially proven benefits of geosynthetics utilized in an unpaved highway. Similar qualitative benefits have been seen for the paved highway with a geosynthetic-reinforced subbase. A majority of highways in Wisconsin crosses soft, frost susceptible soils that typically have been replaced with costly, select, thick, granular material layers. Geosynthetics provide the potential to reduce highway construction costs by partially replacing expensive, thick granular material layers.

2. BACKGROUND

At the base level this report consists of a review and discussion of pertinent literature, collected strain data and falling weight deflectometer tests from three test sections installed along State Highway 45 near Antigo, Wisconsin. Important subtopics regarding general geosynthetic knowledge that was pertinent for this research have been separated below to allow for a clearer understanding of the whole.

2.1 Geosynthetic Types

Currently, many types of geosynthetics are available for purchase world-wide. This research only deals with two main kinds of geosynthetics. These are the geogrid and the geotextile. A geogrid is formed by biaxially stretching a plastic sheet that has numerous small holes punched out of it. This manufacturing process hence defines two key terms, the machine direction (MD) and the cross-machine direction (XD) that will be used throughout the rest of this report. The MD is parallel to the longitudinal (unrolled roll length) direction, likewise XD corresponds to the shorter length and transverse direction. These sheets are stretched to a post-yield condition that provides for a stronger, strain-hardened material and a roll with large apertures. Alternatively, a geogrid can be formed by heat bonding or knitting several strands together in a grid-like pattern. The geogrids are represented by symbols of KGG and PGG, which are characterized in Table 1. Symbols KGG, PGG and WGT were selected for reference ease. The first letter refers to manufacturing process of geogrid (K =

knitted and P = punched sheet drawn) and fabric style of geotextile (W = woven). The second and third letter refers to geosynthetic types (GG = geogrid and GT = geotextile).

A woven geotextile (WGT) is similar to a fabric. It is manufactured by interweaving together numerous yarns in a close-knit pattern. The pattern is tight enough to filter some sand particles, thus an apparent opening size (AOS) typically characterizes the openings of a geotextile. Some of the commonly reported material properties for the geosynthetics used in the demonstration project are shown in Table 1. Figure 1 presents a picture of these specimens side-by-side.

Table 1. Geosynthetic Properties

Specimen	Polymer	Density (mg/cm^2)	Aperture Size (mm) (XD/MD)	Strength [a] @ 5 % (kN/m) (XD/MD)	Flexural Stiffness [b] (mg-cm) (XD/MD)
Grid I (PGG)	PP	23.7	38 / 28	13 / 9	1468 / 1747
Grid II (KGG)	PP	15.3	15 / 15	13 / 9	452 / 579
Textile (WGT)	PP	28.8	0.6 (AOS)	20 / 20	Not reported

PP = Polypropylene
[a] As reported by manufacturer
[b] As reported by Wisconsin Department of Transportation (WisDOT)

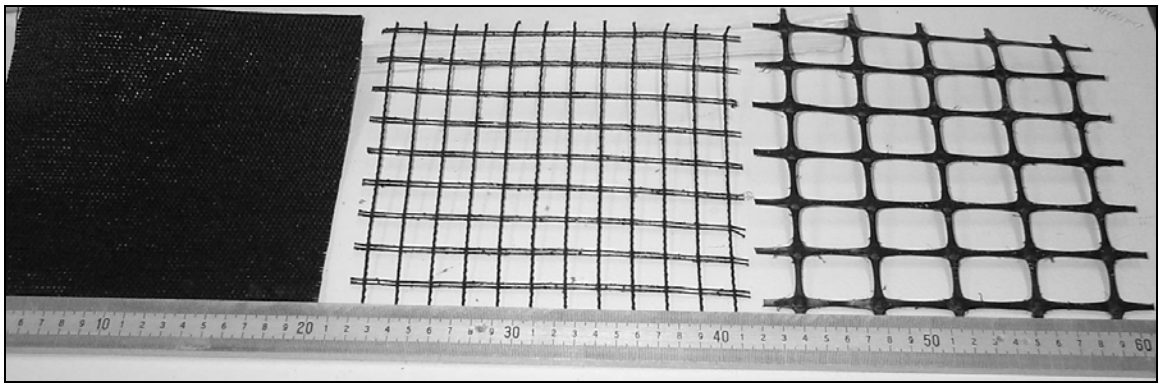

Figure 1. Picture of Geosynthetics: PGG, KGG, and WGT From Right to Left.

2.2 Environmental Issues

A geosynthetic is affected by its surroundings or environment. Environmental factors that contribute to the degradation of geosynthetics include UV radiation (sunlight), mechanical/physical wear, long duration loads, and temperature. A polypropylene textile or grid, such as utilized during this field experiment, will creep when exposed to tensile loads. A creep coefficient between 0.2 and 0.4 percent per log minutes is reported to be typical at room temperature (Jones 1995). Creep is also enhanced by an increase in temperature. A typical range of surrounding soil temperature of 0 to 16 degrees Celsius is greater than the glass transition temperature (T_g) of polypropylene. When the temperature is greater than T_g, a visco-elastic behavior is observed. At temperatures below T_g an elastic behavior best describes the material's response. Additionally, UV radiation in sunlight can cause serious degradation and weakening of polymer bonds. However, about two percent carbon black, which adds the black color to the polymer, is added to absorb UV radiation and to

counteract (resist) degradation due to sunlight. Finally, a design factor, which accounts for mechanical/physical wear during installation, should be utilized in the design process to account for degradation (Jones 1995).

2.3 Highway Applications

There are many applications of geosynthetics. Even within the highway application of geosynthetics, further division is necessary for clarity. Geosynthetic highway applications can be split into two areas, which are unpaved and paved roads. It is important to distinguish between the two, since different theories, physical mechanisms, design methodologies and failure criteria are utilized for each.

2.3.1 Unpaved Road

An unpaved road is of concern for the U.S. military, forest service, logging industry, and other organizations that must traverse and haul loads across undeveloped terrain. Typically, such grades are crossed with a minimum amount of preparation that allows for an efficient movement of relatively few, but heavy, load repetitions. Rutting in the wheel paths is allowed but typically is desired to be four inches or less in depth. Regrading or leveling of the ruts can be performed but is not typically considered for an initial design of a layer of select granular material, which is placed upon the subgrade as a surface course. The purpose of this surface course is to transfer the surface load to the subgrade

while spreading out the load to the subgrade, which effectively reduces the intensity of pressure on the subgrade (Steward et al. 1977).

A geosynthetic placed properly does improve an unpaved road. The most effective location of the geosynthetic is below the select granular material and on the subgrade surface (Das et al. 1998). In this location the geosynthetic provides separation, lateral restraint of the upper granular course and a tensioned membrane effect when strained extensively. A geotextile separates a granular course from a fine-grained subgrade , due to its relatively small apertures or apparent opening size (AOS). However, a geogrid also provides separation due to its less than 100 percent open area and better lateral restraint of upper granular particles. Due to interface friction and interlock with many individual ribs, a geogrid provides superior lateral restraint of the upper granular course, whereas the geotextile relies exclusively on interface friction for lateral restraint (Steward et al. 1977).

The tensioned membrane effect requires that the geosynthetic be extensively strained (i.e., deeply rutted) for this mechanism to contribute a significant benefit. More will be said about this issue in Section 2.4.3.

2.3.2 Paved Road

The other application is the paved road. This application also encompasses the unpaved application since during construction of a paved road relatively few repetitions of trucks heavily loaded with construction materials traverse the partially completed (unpaved) highway grade. This often is a critical

stage. Then, construction is completed with placement of an asphalt surface course, thus the highway is paved and open to the public. The open highway is exposed to many repetitions from loaded truck traffic; however the intensity of subgrade load is considerably less due to the greater stiffness of the surface course. Benefits of an underlying geosynthetic during construction are apparent, but as time and greater numbers of load cycles pass, the benefits are not as clear for the paved road (Barksdale et al. 1989).

Long-term benefits have not typically been assessed for geosynthetics for several reasons. Long-term studies are not particularly conducive to research that is initiated and completed within a time span of a few years. Additionally, there is the issue of survivability of instrumentation and an unwillingness of highway construction administrators to allow for control sections that would serve as a baseline of performance comparisons. Control sections inevitably will under perform reinforced sections, thus requiring additional maintenance and/or premature replacement, which require more money. Lastly, more variables enter into long-term performance studies, thus complicating the issue at hand (Henry 1999).

The purpose of geosynthetics placed below the granular base or subbase of a paved road is to allow for increased numbers of load repetitions prior to failure due to rutting and/or fatigue. Typically, shallow (less than one inch) rutting defines failure for a paved road, since fatigue failure is due more to the internal failure of the asphalt pavement.

The paved road application is a primary concern of the Federal Highway Administration (FHWA) and State Transportation Departments across the United States. Any benefit realized for highways that compose this nation's infrastructure would translate ultimately to monetary savings while providing similar, if not better, performance.

2.4 Geosynthetic Theories and Issues

At this time three theories appear to account for benefits provided by a reinforced geosynthetic subbase. These are: separation, lateral restraint, and a tensioned membrane effect.

2.4.1 Separation

Roadway distress or failure may occur when fines from the subgrade contaminate an overlying granular layer. High stresses transmitted from wheel loads on the surface above, combined with a thaw weakened/saturated subgrade, typically cause a base and subgrade to mix. This mixing causes a reduction in the effective base thickness by reducing the actual modulus of the granular base as well as its physical thickness. Due to wheel loads above, mixing occurs. Mixing is best pictured as granular material pushed down into the soft subgrade and/or soft subgrade pumped up into the overlying granular layer (Tensar Design Manual 1998). Figure 2 shows a schematic that represents both the mixed and separated situations. A separated condition of different layers is

crucial, since a strong base layer is weakened and thinned when fines from the subgrade are mixed in.

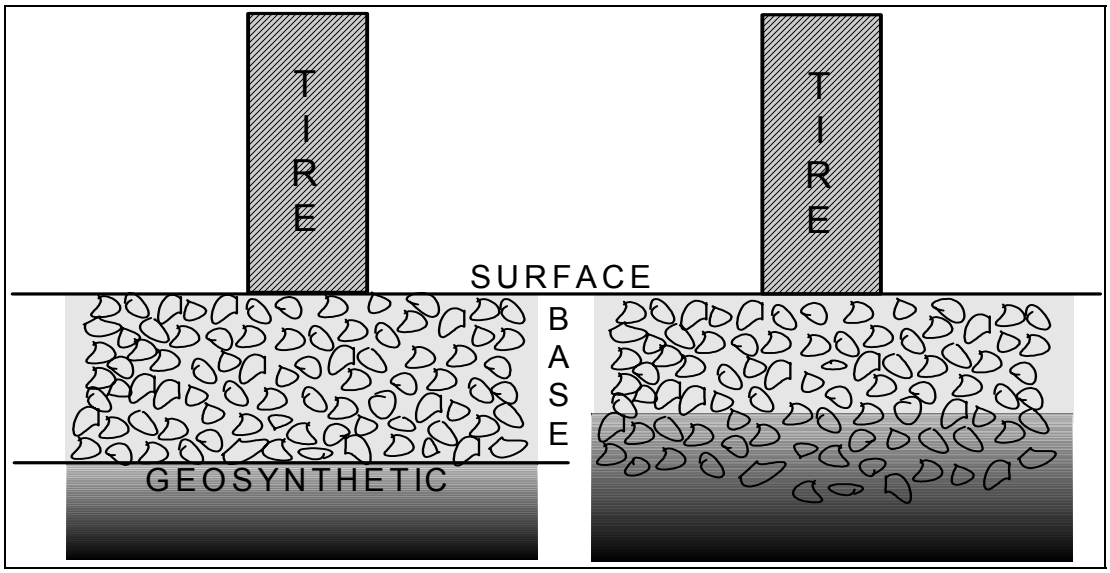

Figure 2. Separation Theory: separated (unmixed), left and mixed, right

2.4.2 Lateral Restraint

This theory is really composed of four related mechanisms that combine to provide better overall pavement performance. First, a shear force is generated at the base of the granular layer as the material would like to move down and out from wheel loads on the above surface. This shear stress is absorbed by the stiffer geosynthetic, thus reducing lateral strain in the upper, granular layer. However simultaneously, this induces a slightly greater lateral stress in the lower portion of the granular layer, thus leading to higher elastic modulus for the granular layer due to the slight increase in confining stress. Therefore, the

granular layer with a greater modulus spreads the surface load over a wider area, thus decreasing the intensity of vertical stress, which implies less vertical strain in layers above and below the geosynthetic. Finally, shear stress absorbed by the stiff geosynthetic transfers less intense shear stress to the subgrade, thus the subgrade is exposed to less, overall stress when also considering lower vertical stresses, as mentioned before (Tensar Design Manual 1998). Figure 3 shows a visual diagram illustrating this.

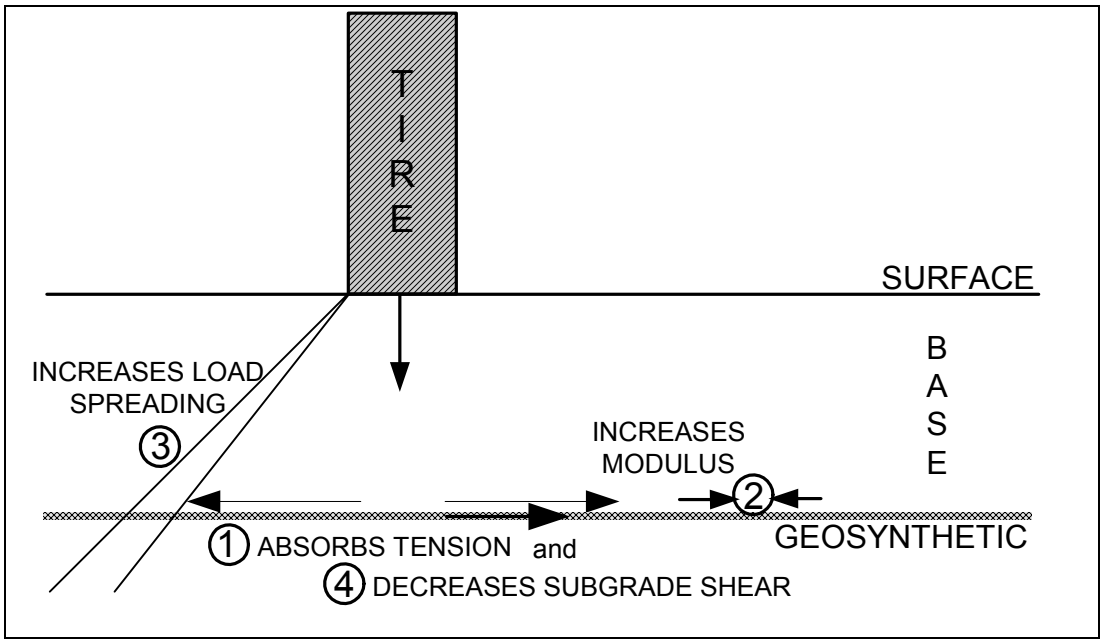

Figure 3. Lateral Restraint Function Showing Four Mechanisms of Improvement.

2.4.3 Tensioned Membrane

The tensioned membrane theory, as described first by Giroud (1981), is more relevant when a rut or large (greater than 25 mm or 51 mm) vertical deformation is allowable. Thus, this theory is relevant to the unpaved road.

Simply put, the tension in a highly distorted membrane at the base of an overlying granular layer provides a reaction with a vertical component that contributes to supporting the wheel load at the surface and confines the soft subgrade below. Again however, significant strain, which is unacceptable for a paved road, is required for the tension membrane mechanism to contribute benefit (Tensar Design Manual 1998). Figure 4 schematically shows the described force/mechanism.

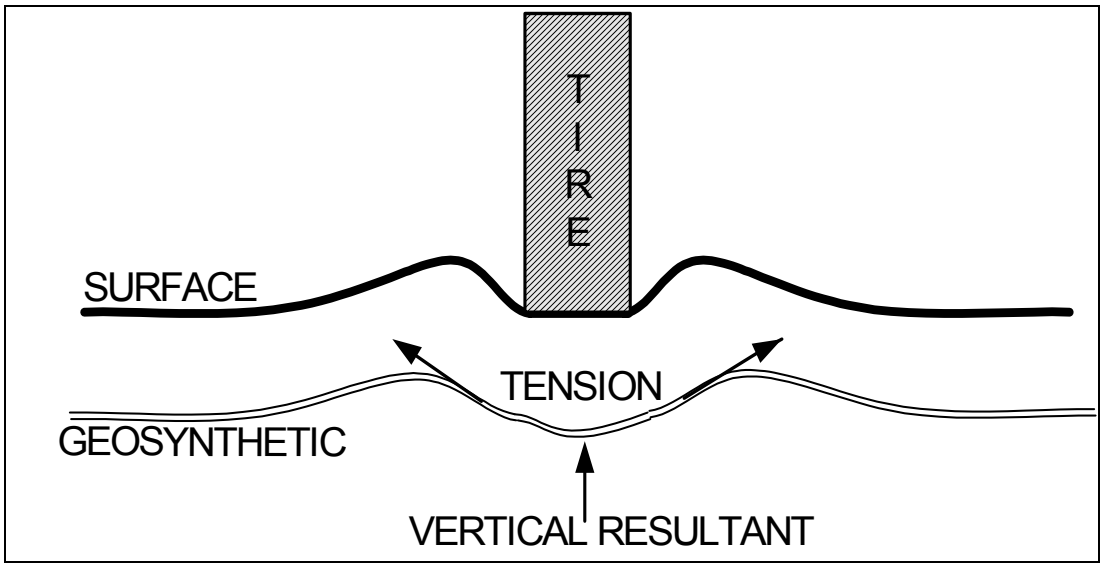

Figure 4. Tensioned Membrane Function Showing Displacement and Resultant Force.

2.4.4 Modulus at Low Strain

Another important issue is that of determining or utilizing an appropriate modulus value for purposes of design. Many tests (i.e., biaxial, uniaxial, confined (triaxial), repetitive loading) have been performed to replicate stress and strain conditions in the field. However, more field experiments are necessary to

establish which laboratory determined modulus is most appropriate for design purposes. Currently, modulus values for geosynthetics are widely published when strain equals five percent (Austin et al. 1993). This appears to be similar to strain levels observed in field experiments where geosynthetics are employed for unpaved road applications (Henry 1999). However, limited field experiments show cumulative strains of less than one percent for a typical geosynthetic used below a subbase of paved road applications. Additionally, observations for a paved surface indicated that the best location for a geogrid is where radial elastic strains under the dynamic load center range from 0.05 to 0.2 percent strain (Haas et al. 1988).

2.5 Design Methodologies

Several design methodologies have emerged since the late 1970's that address geosynthetic reinforcement. Reviews of significant work relating to design methods indicate two that warrant further discussion. These methods were presented by, the following authors: (1) Barenburg, Dowland, and Hales (1975) and (2) Giroud and Noiray (1981). These different theories were chosen since both are original works that have contributed greatly to a better understanding of geosynthetics when used in roadway applications. Many other design methods exist (i.e., manufacturer guidelines) but most are based on Barenburg et al. (1975) theory.

2.5.1 "Barenburg" Method

Barenburg et al. (1975) presents a method that utilizes different bearing capacity factors for the unpaved road application with or without a geotextile. "Lateral restraint theory" is at the core of this method. Soft, cohesive soils were assumed to compose the subgrade. Load repetitions of less than 100 are assumed. A granular surface course layer consists of crushed-rock aggregate with minimum thickness. The research by Barenburg et al. (1975) based on small-scale laboratory tests showed that bearing capacity factors (N_c) of 6 and 3.3 were appropriate for loading with and without the inclusion of a geotextile placed upon the subgrade, respectively. Currently, the United States Army utilizes the same approach for construction of low-volume unpaved roads with minor design improvements provided by Steward et al. (1977) and Henry (1999). The simple design procedure is as follows:

(1) Determine an equivalent cohesion (C) for the subgrade soil, often based on undrained shear strength.

(2) Determine a maximum wheel load.

(3) Choose the appropriate bearing capacity factor (N_c), where N_c = 6 (geotextile included) and N_c = 3.3 (no geotextile).

(4) Calculate the allowable bearing pressure on the subgrade (p_a), where $p_a = C(N_c)$ for each case and C = cohesion as well as Factor of Safety = 1.

(5) Determine the crushed-rock aggregate thickness for each case utilizing the correct design chart, based on the expected maximum wheel load and both allowable bearing pressures.

(6) Choose a geotextile based on installation damage factors and other environmental criteria, and determine its cost.

(7) Evaluate both proposed sections to determine the less expensive one.

Further examination of the Barenburg et al. (1975) method indicates that a circular contact area is assumed and a Boussinesq stress distribution determines stress at a given depth below the surface. The bearing capacity factors determined are interesting. As described in proceeding paragraphs, $N_c = 6$ when a geotextile is used and $N_c = 3.3$ when it is not used. Earlier research by Rodin (1965) indicates that at the onset of localized bearing failures $N_c = 6.2$ for a rigid, surface footing and $N_c = 3.1$ for a flexible footing. Apparently, the addition of the geotextile upon the subgrade causes the section to fail similar to that of a rigid footing, which displays general bearing capacity failure rather than local bearing capacity failures. Additionally, the Barenburg et al. (1975) method was extended to address a slightly greater number of load repetitions by Steward et al. (1977) through further reductions of the recommended bearing capacity factors.

Barenburg et al. (1975) design method does not utilize the modulus or tensile strength of the geotextile for any purposes. With the advent of stronger (high modulus) geosynthetics and observations of apparently better performance, the effects of modulus could no longer be overlooked. Thus, another method that accounts for modulus was needed, which led to the following design approach presented during the 1980s.

2.5.2 "Giroud" Method

Giroud and Noiray (1981) presented the first method that utilizes a geotextile's modulus or tensile strength to determine an equivalent section thickness compared to a section without a geotextile. Giroud and Noiray (1981) assumed a soft, saturated clay subgrade that is undrained. The near surface granular material, if any, is assumed to have a California Bearing Ratio (CBR) of at least 80. Unlike Barenburg's method, a zero thickness of the granular surface course or placement of only a geosynthetic is possible when applying this method.

Giroud and Noiray (1981) initially follow the same "lateral restraint theory" that Barenburg et al. (1975) proposed, but add to this a "tensioned membrane theory," which is a function of the geotextile modulus. Other differences include using a rectangular shaped contact area and a very liberal stress distribution. The resulted overall effect of the "tensioned membrane" theory, a different shaped contact area, and a liberal stress distribution can recommend thin granular surface course layers when high modulus geotextiles are utilized, as compared to Barenburg's design method.

Comparison by Henry (1999) clearly demonstrates differences between Giroud and Barenburg methods. Additionally, a new design approach that incorporates a Boussinesq stress distribution with the Giroud design method is recommended. Further research that addresses the effects of contact area shape and stress distribution in granular materials other than crushed aggregate is also recommended (Henry 1999).

3. FIELD METHODS AND MATERIALS

The field demonstration consisted of installing and observing three demonstration test sections, as part of a geosynthetic-reinforced subbase placed during State Highway 45 reconstruction. Therefore, the following methods and materials are pertinent to either the background context or the field demonstration.

3.1 Application And Mechanisms

Preparations for installation of three separate geosynthetic trial sections began in August 1999. Shortly before this, the Wisconsin Department of Transportation (WisDOT) provided information about a current construction project where geosynthetics were planned to reinforce the subbase. Hence, this project was chosen by the UW-Madison as a demonstration site to experiment with strain gage instrumentation on geosynthetics. Strain gages were ordered, installation procedures using epoxy was studied and a literature review begun. The field demonstration consisted of monitoring 30 strain gage pairs installed on the geosynthetic trial sections placed below the subbase layer along State Highway 45 near Antigo, Wisconsin.

3.2 Geosynthetic Selection

The contractor, based upon specifications provided by the Wisconsin Department of Transportation, determined the geosynthetics to be utilized. The

intent of the specifications was to have a stiff geogrid, a flexible geogrid and a woven geotextile utilized during construction. However, due to ambiguity of ASTM D-1388 specification, the contractor was allowed to utilize two different geogrids that were both essentially flexible. See Table 1 for the properties of the three geosynthetics.

3.3 Strain Gage Selection

Gages were selected after reviewing information provided personally from Dr. Khalid Farrag, P.E. (1999). Also, tech tips 605 and 607 by Measurements Group, Inc. (1993) were reviewed. An open-faced cast polyimide backing (E) was chosen due to its flexibility. The grid foil consisted of annealed constantan (P) alloy. Hence, these choices indicate an EP-type strain gage provided by Measurements Group as the appropriate gage for this application. A geosynthetic constructed of plastic has the ability to elongate excessively, thus a high elongation gage was deemed appropriate. The EP gage has an electrical grid constructed of very ductile, annealed, constantan alloy. Additionally, this gage minimized the amount of thermal drift due to resistive self-heating. The model number of the selected gage was EP-08-250BG-120. The resistance of the gage is 120 ohms. The length and width of the gages are 6 and 3 millimeters, respectively.

3.4 Strain Gage Attachment

A prior description of similar strain gage attachments as provided by Farrag (1999), was reviewed and followed. In summary, the first step was to apply the strain gage to the geosynthetic after etching the surface with a light abrasive cloth. Next, the abrasive surface was cleaned with a weak acid conditioner (MM Conditioner A). Then, a weak base (MM Neutralizer 5A) was used to neutralize and thoroughly clean. The prepared surface was finally dried with clean gauze and allowed to air dry completely before applying a gage.

The bondable gages were applied using a two-part epoxy, pressure and a cure period. The A-12 adhesive was mixed together using a 2:3 ratio of part A to part B. Once mixed, the epoxy was applied to the backside of the strain gage, which was then pressed onto the prepared surface. Pressure was held on the gage during the cure period by clamps or dead weights. Two different curing schedules were adhered to, based on the physical size of the geosynthetic specimen. Laboratory specimens (200 x 200 millimeters) were clamped at approximately 140 kN/m^2 and cured for at least 2 hours in an oven set at 75 degrees Celsius. The geosynthetic, partial-roll sections used in the field experiment were held in place with lead weights (approx. 70 kN/m^2) and cured for two weeks at room temperature (approx. 21 °C). Additionally, terminals were bonded and clamped to the geosynthetic at the same time as the gages. The model number of the terminal strips used was CPF-50C.

3.5 Weatherization

This application puts strain gages in a most severe environment. In the field, the gages must be protected from moisture and physical damage while maintaining flexibility to accurately measure small strains. For the field demonstration a procedure similar to Dr. Khalid Farrag's (1999), was followed. Weatherization procedures for strain gages in this demonstration were:

(1) Terminals and lead strands were coated with polyurethane.

(2) Teflon film was wrapped around or placed over the gages.

(3) FBT butyl rubber encapsulated the gages and Teflon.

(4) Aluminum foil was applied to the FBT butyl rubber coating.

(5) A nitrile rubber coating, which is slightly more durable than FBT butyl rubber, was applied to the aluminum foil layer as a final coating. Occasionally more than one coating was applied to insure adequate coverage.

Particular attention was given to the wire leads that extend from the weatherization coatings. Each rubber layer completely covered the entire circumference of each wire.

3.6 Test Section Orientation

Three test sections, each approximately 7 meters in length and a roll width wide, were installed end-to-end in front of the residence of Michael and Elsie Losser. All test sections were placed below the outside lane of the two southbound traffic lanes of State Highway 45. The individual test sections are

aligned in a north-south direction, in order from south to north: PGG, KGG and WGT. Figures 5, 6 and 7 show the location according to stationing and orientation of the strain gages and sections placed.

Within each block shown in Figures 5, 6 and 7 that indicate “location of strain gages,” four strain gages are installed. Strain gages are placed opposite each other (top and bottom) on the geosynthetic, forming a set to compensate for localized bending. Additionally, another strain gage set was placed nearby, mounted in an orthogonal direction. However, an exception occurs for the KGG section, where each block location only contains a single set of strain gages placed in a direction that is perpendicular to the southbound traffic lane. Gages could not be mounted in the parallel direction for KGG section since that orientation consisted of only a one composite strand, which was expected to cause problems due to a strand width being smaller than that of an applied gage. In summary, strain gauges were installed on each section to collect information from 6 local areas, which include orthogonal orientations, for PGG and KGG sections. Thus, a total of 30 individual locations were instrumented.

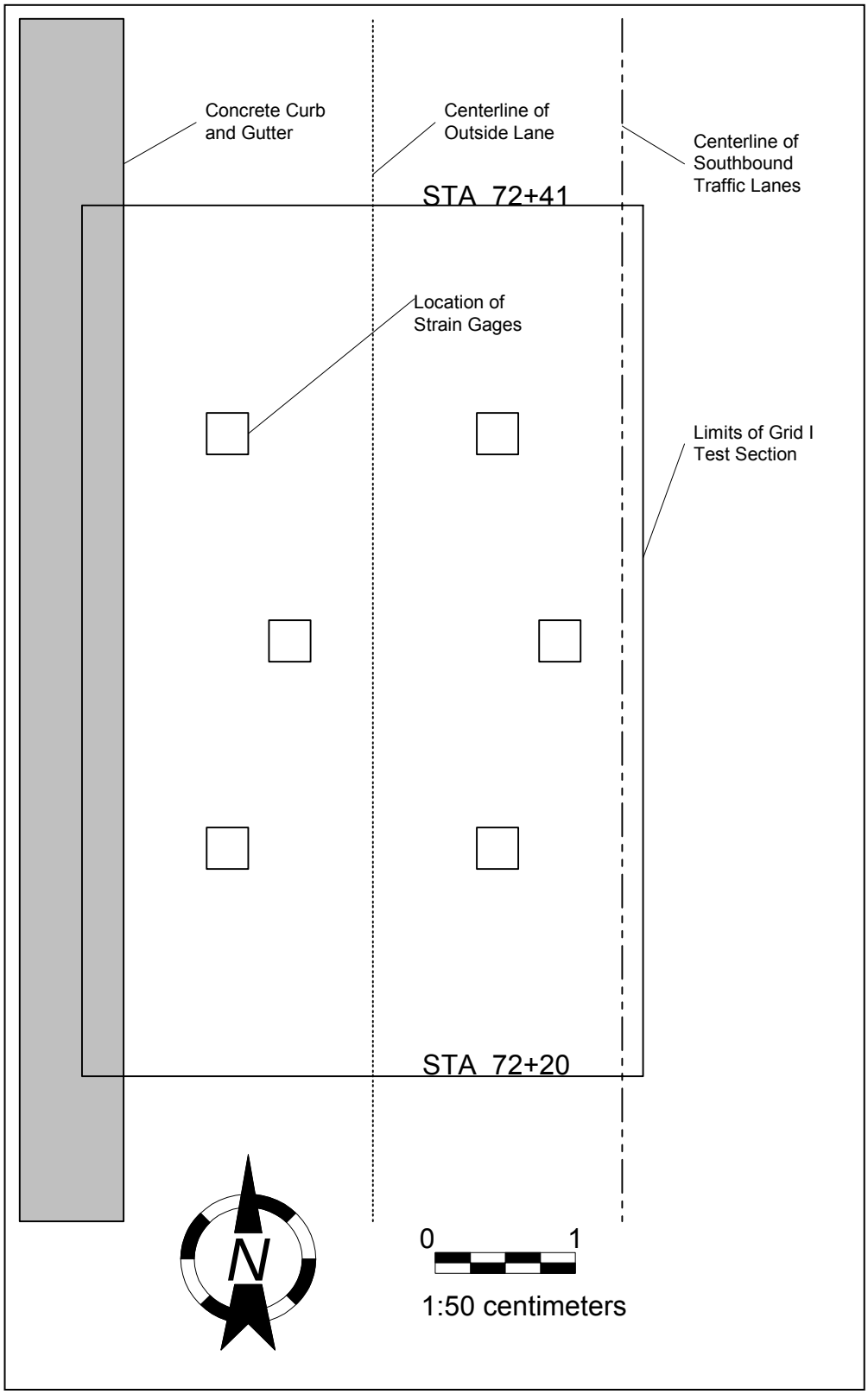

Figure 5. PGG Section Showing Strain Gage Location and Orientation.

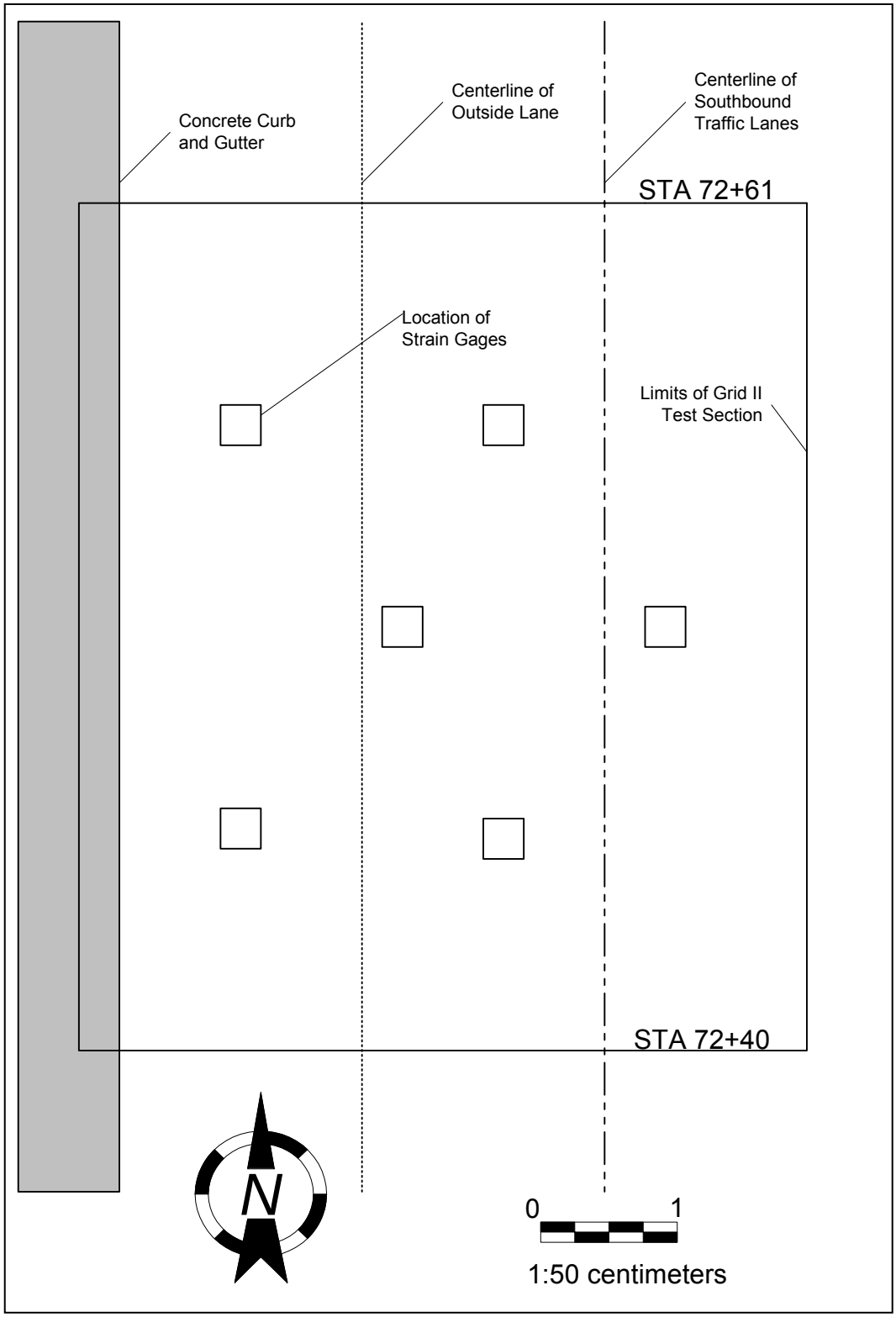

Figure 6. KGG Section Showing Strain Gage Location and Orientation.

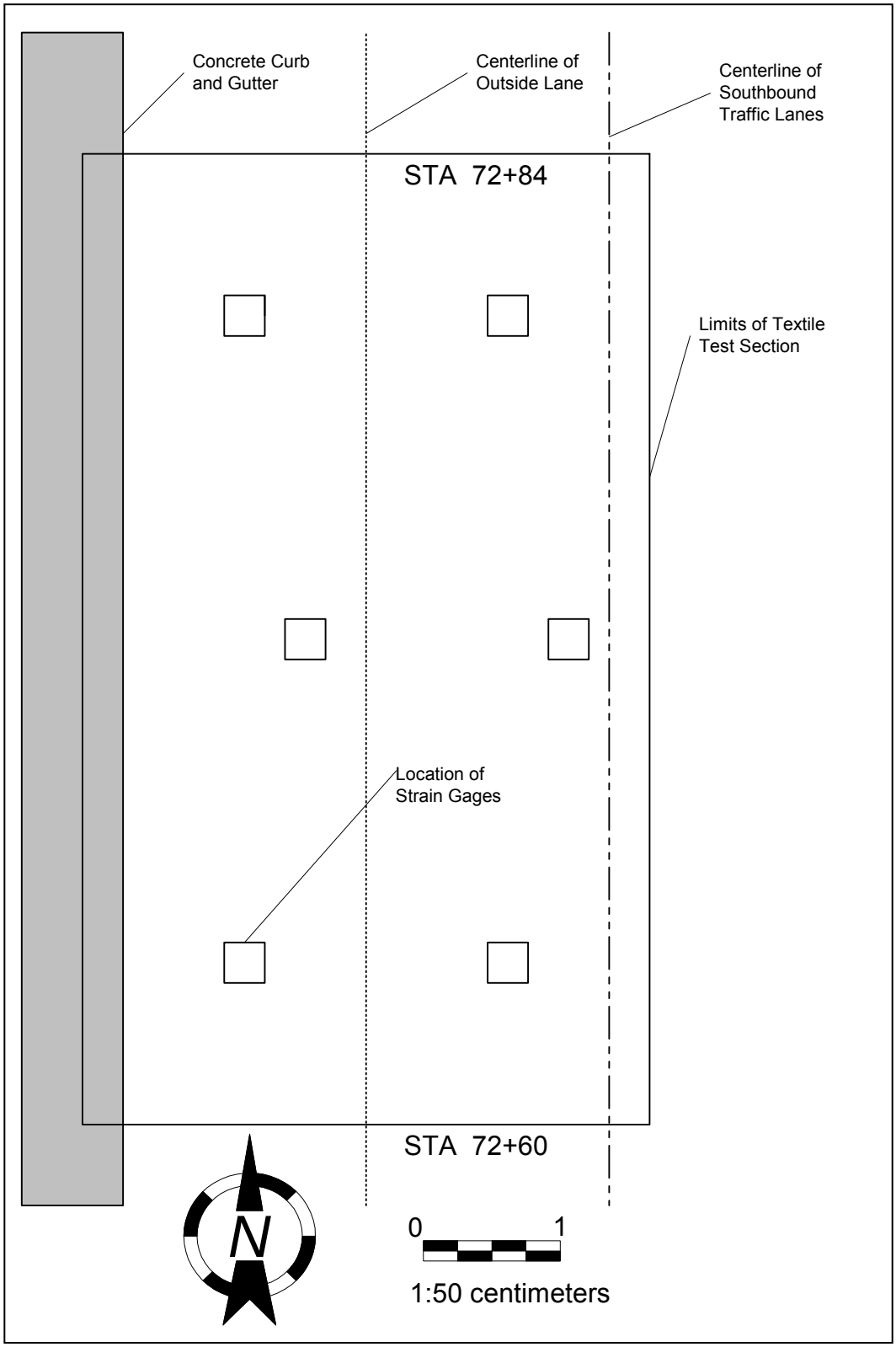

Figure 7. WGT Section Showing Strain Gage Location and Orientation.

3.7 Data Collection

Data collection was accomplished using a CR-10 Campbell Scientific data logger, a desktop computer, generator, battery and precision resistors for electrical circuit completion. The electrical circuit, which cancels bending strain, is shown in Figure 8.

Percent strain was calculated based on the geometry of the circuit, known resistance and the gage factor of the strain gages. The following equation was used to determine the percent strain. Strain (%) = $-2 * V_o / 1000 * \{1+(0.1/120)\} / 2.06 * 100$.

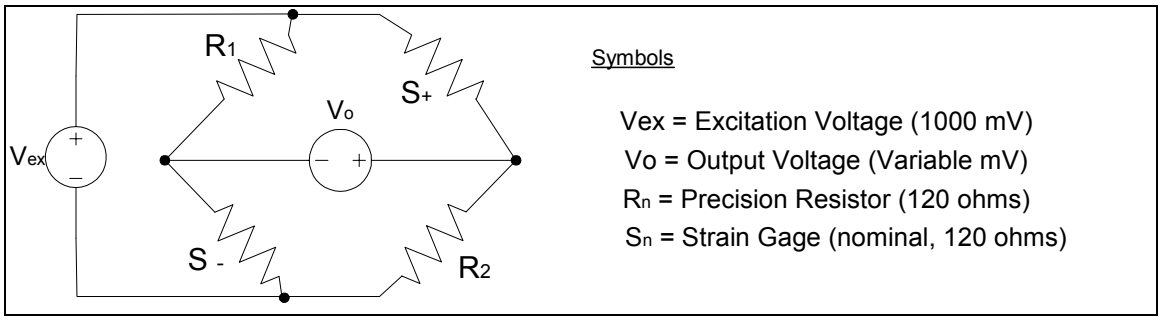

Figure 8. Schematic of Electrical Circuit showing connections that cancel bending strain.

The data collection system was loaded into a Chevrolet Suburban for on-site mobility and to haul the equipment to the Antigo demonstration site. Data collection was performed several times during and after construction of the highway. The first strain gage observations (readings) were used to initialize or zero all gages prior to placement of the granular subbase layer.

3.8 Temperature Correction Of Gage Measurements

Strain gage readings were collected in the field during the months of September, October, December and March. Obviously, the surrounding soil and gages were not always at room temperature (21°C). Thus, a correction was necessary to express the field data at one given temperature for later temperature independent comparisons. Laboratory relationships were determined through tests that allow for correction of all field measurements to room temperature. The in-place geosynthetic temperature should have been sensed using thermocouples. For this same purpose however, a finite-element analysis was performed using Temp/W computer software. Soil properties and average daily air temperatures were used to accurately estimate the subsurface temperature at the subbase-geosynthetic interface. Representative thermal soil properties were obtained from UWFROST literature (Bosscher et al. 1998).

3.9 Strain Gage Calibration

Strain gages are intended to measure local strains. For the geogrids this local strain equals that of the ribs between junctions. The strain gage width approximately covers the entire rib width of the geogrids, thus the gages were expected to measure the overall, local strain of a single rib quite accurately. The geotextile was composed of numerous smaller strands that further complicated strain measurement. Literature indicates that a gage should measure 25 to 100 millimeters in length when installation on a geotextile is planned (Farrag 1999). However, the gage supplier, Measurements Group, required approximately eight

weeks to manufacture and deliver large (25- to 100-millimeter) EP type strain gages. Such time was not available prior to placement of the instrumented test sections. Therefore, the small six-millimeter length gages were applied to the geotextile, since the alternative was not to apply any gages to the geotextile. When measuring strain of a geotextile, a gage that spans more strands should provide a more representative strain, which is less affected by action or non-action of a single small strand. However, strain gage calibration relates an actual or extensometer strain to that measured by the strain gage. All geosynthetic applications utilized in this demonstration were calibrated to establish their relationship to actual strain, as measured by an extensometer in a controlled laboratory environment.

Geosynthetic samples were removed (cut) from the partial-roll portions of the materials used for the field experiment. Samples, 200 by 200 millimeters, were cut. Next, strain gages and lead wires were attached. Finally, a 25-millimeter long extensometer was located directly above the strain gage and attached prior to calibration testing.

A tension machine was used to test the geosynthetic specimens. Uniaxial, unconfined tension tests were then completed similar to ASTM D 4595, Wide Width Tensile Test. The relationships measured are reported in Figures 9 and 10 for the geogrids and geotextile, respectively. Data for these relationships was collected on nearly a continuous basis, so the typical data point collection symbols, as shown, should only be used to distinguish between different tests.

Also, note that only the XD machine direction of KGG is reported due to the earlier mentioned reason in Section 3.5.

Figure 9a shows that a 1:1 calibration curve exists for the geogrids at low strain levels, which covers the range of strains observed in the field. However, Figure 10a shows a calibration relationship for the geotextile that requires correction of the observed field strain. Visual observations during the laboratory calibration tests indicate that only a couple strands of the geotextile were perhaps bonded to the gage.

The next step of the calibration process was to determine an apparent load contribution based on the temperature corrected extensometer strain measurements for each of the geosynthetics. This was completed using the laboratory-determined correlations between apparent tensile load and extensometer strain. These correlations are shown in Figures 9b and 10b for the geogrids and geotextile, respectively.

An average value that exists between two replicate tests was used for both geogrid types (Figure 9b), since these relationships appear to be unique and consistent for each type and orientation. However, the correlations for the geotextile doesn't produce such unique, consistent curves as Figure 10b shows. The slopes of the individual curves, which may be called stiffness in Figure 10b, do appear to display trends. These individual trends shown for three replicate tests were averaged between one and two percent extensometer strain where trends appear to be somewhat consistent. The average trends were then used to correlate strains to apparent tensile loads for both orientations. Laboratory

observations indicate that individual trends vary due to take-up at the beginning of the tension tests. The consequence of the geosynthetic slack is a shift in the location of the origin. Other researchers have experienced and reported similar problems (Austin et al. 1993).

3.10 Falling Weight Deflectometer Test

A falling weight deflectometer (FWD), an in-situ non-destructive testing device, was observed to provide an alternative performance evaluation. WisDOT owns and operates a single FWD machine, mainly for inventory purposes of highways throughout Wisconsin. This Kuab 2m-33 was utilized to collect the FWD data during this field experiment. The machine is mounted on a two-wheel trailer, which is towed by a specially equipped truck. The support truck contains computer controls, a data collection system, and a printer to provide immediate results when needed. Figures 11 and 12 show both side views with respect to the front of the FWD equipment.

The Kuab 2m-33 delivers a load to the pavement through a segmented plate, which provides contact with the ground surface. The 2 m designation in the model name signifies that 2 masses combine to provide the total load. First, the segmented plate and loading frame provide static preload to the pavement. Secondly, a falling weight from a different height provides the larger portion of the total load. The maximum capacity of the machine is achieved when the maximum mass is dropped the full height.

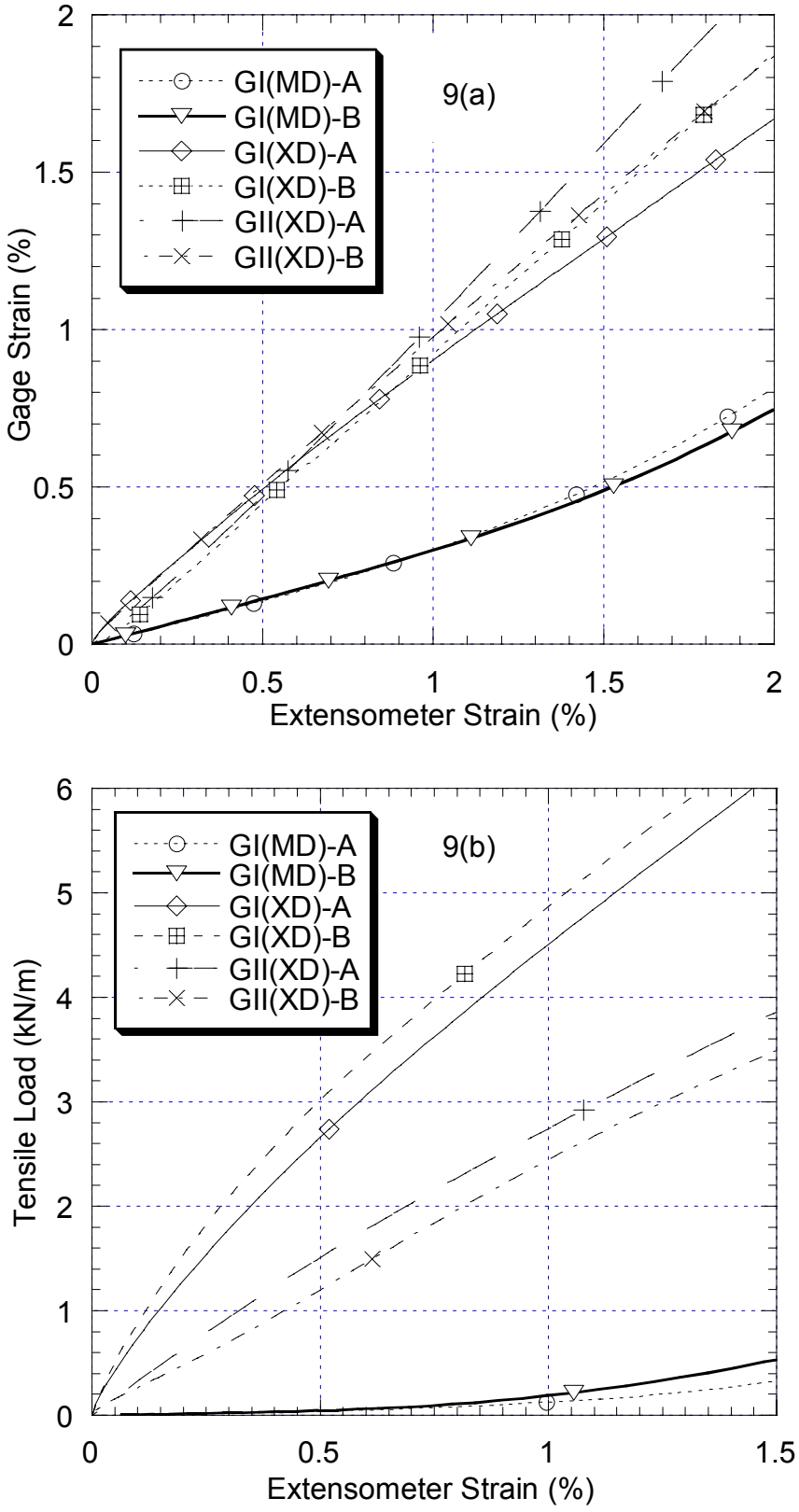

Figure 9a and 9b. Calibration and Correlation for Geogrids

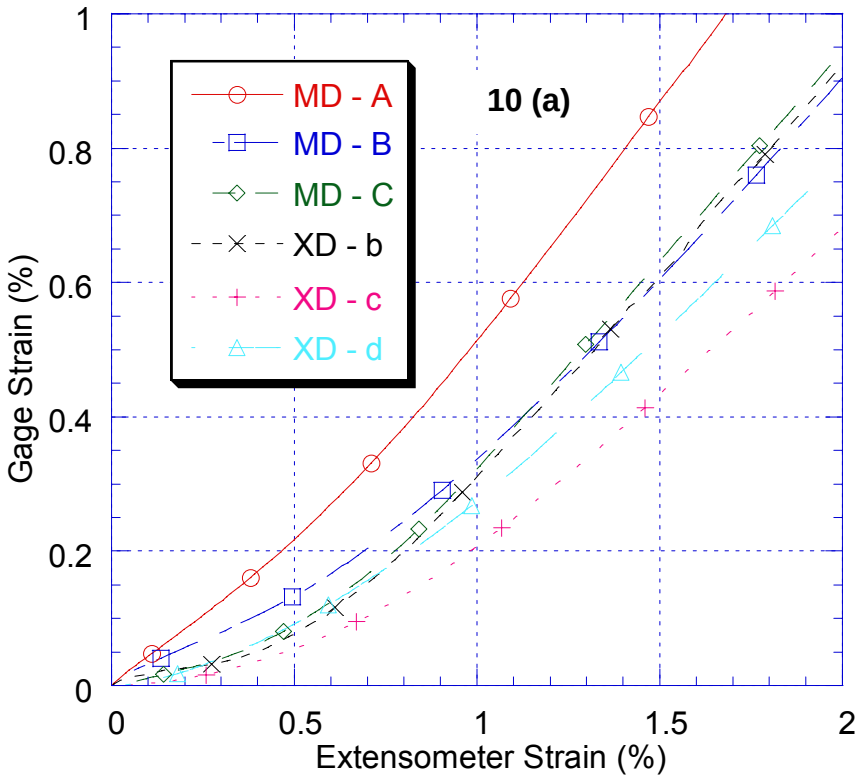

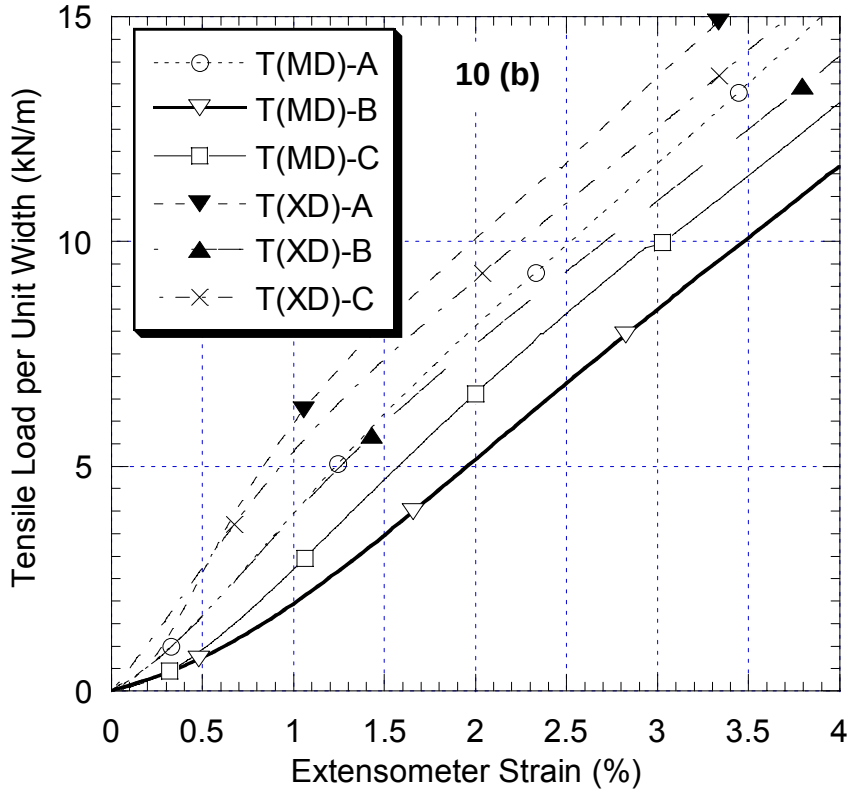

Figure 10a and 10b. Calibration and Correlation for Geotextile

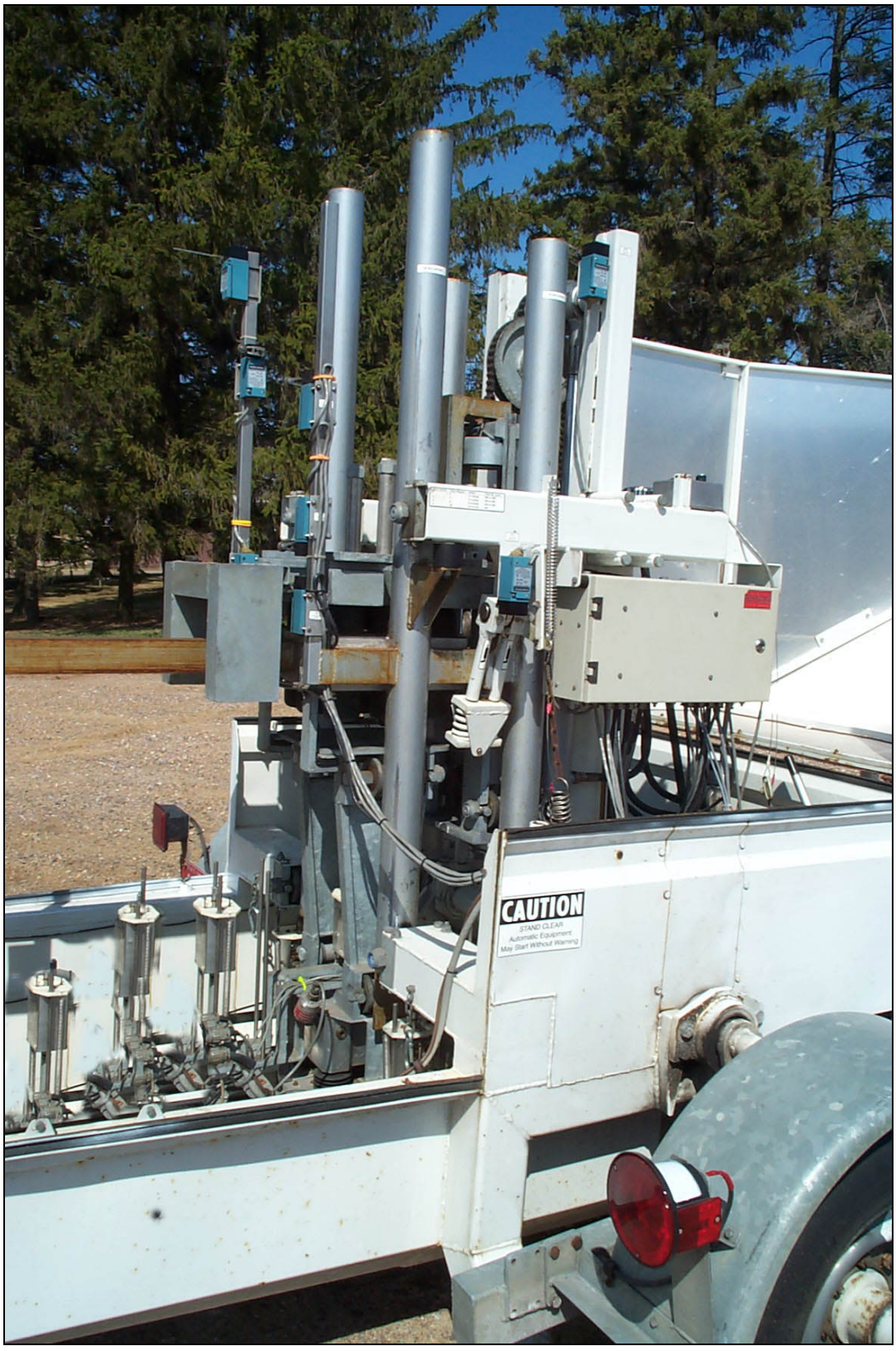

Figure 11. Right-hand Side View with respect to Front of the FWD Showing LVDTs and Load Frame.

Figure 12. Left Side View with.respect.to. Front of the FWD Showing LVDTs and Segmented Plate.

For the demonstration, FWD data was collected along the southbound alignment length of 125 meters, which spans the three demonstration sections. Station intervals varied between 1.5 and 6 meters, however, tests performed on different dates utilized the same spacing. To understand the effect of seasonal changes on pavement stiffness, FWD tests were performed in fall (October 22, 1999) immediately after construction was completed, in winter (December 8, 1999) after the pavement had completely freezed, and in the following spring (March 31, 2000) after the pavement had thawed.

Applying a sequence of loads that increased in magnitude tested an individual station. After applying a 22 kN seating load, the observed load sequence (22, 40, 62 and 80 kN) was completed. Deflections were observed at the center of the segmented load plate and at offsets behind the center with respect to the truck and trailer orientation of 300, 460, 610, 910 and 1220 millimeters, as measured by linear voltage displacement transducers (LVDTs). These deflections, when viewed in profile, create a deflection basin surrounding the point of load. Deflections vary and depend mainly on the asphalt temperature and moisture content of the lower granular layers. Greater deflections are typical during the spring, due to warm and wet conditions that prevail.

A composite modulus is routinely determined and analyzed when evaluating the non-linear behavior of the pavement section. This composite modulus is that of a homogeneous, elastic half-space, which would provide the same deflection at a given radial distance when the same force and geometry

are applied. Hence, material at greater depth is observed by LVDTs at greater radial distance from the load center. A linear material will have constant composite modulus with increased radial distance/depth.

Non-linear materials such as layered pavement sections will have a variable composite modulus with increased radial distance/depth, due to differences of moduli and greater confining stress with increased depth. The variable, non-linear composite moduli calculated for this demonstration project correspond very closely with the different material types and depths that make-up the pavement section.

3.11 Modulus Back-calculation

MODULUS 5.0 software from the Texas Transportation Institute (TTI) was utilized to back-calculate layer moduli through an iterative process. This software determines moduli of the individual layers based on elastic layer theory and known surface deflections in response to a static load. Additional input consisted of observed equipment geometry and layer thickness as well as assumed Poisson's ratios. Poisson's ratios of 0.35, 0.35 and 0.40 were assumed for the asphalt, granular materials and the low plasticity, fine-grained subgrade, respectively.

Initially, moduli values for all layers were back-calculated allowing MODULUS 5.0 to iterate to find the value that provided for the best-fit model compared to the observed deflection basin. Based on these results and engineering judgment, typical values were selected for the hot-mixed asphalt

pavement, base course and subbase. The initial back-calculated modulus values from the latter part of 1999 (specifically, October and December) were given more weight, as other researchers indicate that such values better represent an effective yearly modulus for earthen materials (Bosscher et al. 1998). The asphalt layer is the exception, which is quite dependent on ambient air temperature and solar radiation. Two sources were pursued to estimate asphalt moduli values, which are reported in terms of megaPascals (MPa). First, a theoretical approach was tried using published analytical equations (Huang 1993). This relationship, as determined by the Asphalt Institute, relates predominantly temperature and other variables to the modulus value. Based on the specific superpave asphalt mix design placed for State Highway 45, the relationship indicates a modulus value that ranges greatly from approximately 7000 to 21000 MPa (Huang 1993) over a range of temperatures expected in Wisconsin. These are high values, on the order of ten times greater than what is considered typical asphalt moduli. Secondly, an asphalt modulus, as determined in the laboratory, indicates a value near 1100 MPa for a similar superpave mix design (Christensen 1999).

MODULUS 5.0 was indicating initial backcalculated values of near 20,000 MPa, which again is considerably higher than typical. AASHTO design recommendations typically assume an asphalt modulus between 1500 to 3100 MPa for new pavement construction. Thus, based on this knowledge and engineering judgment, moduli range for asphalt was chosen to be 3100 and 11000 MPa, respectively, for warmer and colder temperatures. These values are

more typical. Additionally, MODULUS was run using high and low modulus values for the asphalt layer and surprisingly the iterative calculation of the subgrade modulus didn't change that much. Thus, the lower, more typical asphalt moduli were used during the iterative process to calculate the subgrade moduli along the project's stationing.

Moduli were also determined for the lower granular layers, which are the base course and subbase. Typical values indicate a range of 70 to 690 MPa (Huang 1993). The initial backcalculation provided values within this smaller range. Notably less variability was observed when compared to the asphalt. Therefore, the initial backcalculated moduli were evaluated and values closely corresponding to the initial average values were selected and fixed for later backcalculations. Also, a depth to stiff layer was chosen at 6.0 m for uniformity and to represent the more typical fall months.

Using the more typical moduli and depth to stiff layer, assumed Poisson's ratios and measured layer thickness, final back-calculations were iterated to determine the modulus of the subgrade that would provide the best-fit between calculated and measured deflection basins. A subgrade modulus value of near 30 MPa was used in the simulation. The Shelby tube (76 mm diameter) sample was collected from below WGT test section and the unconfined compression test was performed on September 2, 1999. The correlation of an unconfined compressive strength and strain for Antigo silt loam subgrade is shown in Figure 13.

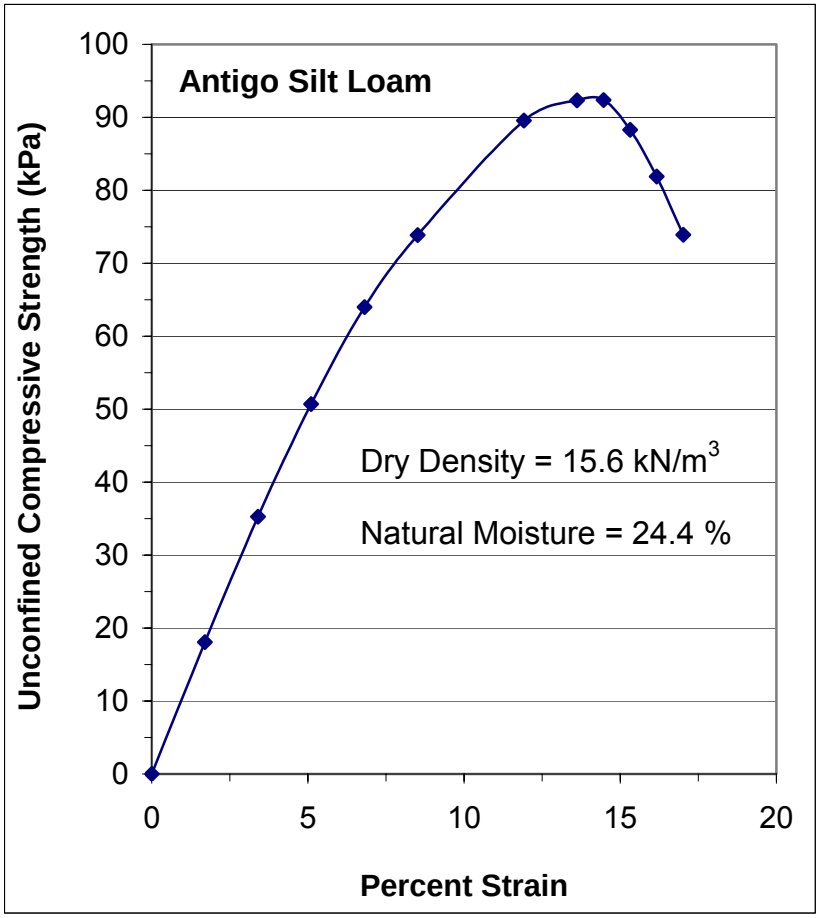

Figure 13. Unconfined Compressive Strength, Antigo Silt Loam.

The backcalculation process generally follows the procedures utilized for the Strategic Highway Research Program (SHRP 1993). SHRP guidelines were established based on several years of backcalculation experience by others. Additionally, U.S. Army Corp of Engineers Technical Manual 5-822-13 and ASTM D 5858-96 were consulted to provide additional recommendations based on their experiences.

4. RESULTS

Strain data results were obtained by applying laboratory-determined corrections and calibrations to the collected strain data. Additionally, analysis and results follow for FWD tests that were simultaneously performed during data collection trips to Antigo.

4.1 Strain Gage Observations And Results

Strain data was collected starting on September 1, 1999, when the geosynthetic test sections were first placed. An analysis, which utilizes laboratory results, was performed on the collected field strain data. The analysis consisted of the following five steps: 1) collect strain readings from gages installed on test sections, 2) correct these strain readings to 21° C, 3) correlate the temperature-corrected strains to extensometer strains using gage calibration curves, 4) using calibration curves determine an apparent load per unit width for each type of geosynthetic and 5) compare the apparent load contributions for the different types of geosynthetic. Table 2 summarizes the processed numerical data for the actual demonstration project. An average value was determined for the cumulated strain data for a period of the 77 days (September 22 – December 8) immediately following the construction of the pavement section where strain levels appeared to have leveled off. Static load tests were completed using the weight on the steer axle and tires of a fully loaded, quad-axle dump truck for a reaction. The truck tires and axle were positioned above the location of select strain gages, and strain observations were recorded.

Table 2. Strain Data Summary.

TEMPURATURE-CORRECTED FIELD STRAINS		
Specimen	Average Cumulative Percent Strain (77 day span, XD/MD)	Max. Incremental Percent Strain Response to a Static Load (58 kN) (XD/MD)
PGG	0.14 / 0.20	0.03 / 0.05
KGG	0.38	0.07
WGT	0.41 / 0.31	0.08 / 0.04
EXTENSOMETER STRAINS AT 21° C (XD/MD)		
PGG	0.37 / 0.70	0.03 / 1.5
KGG	0.38	0.07
WGT	0.76 / 0.48	0.15 / 0.06
APPARENT TENSILE FORCE PER UNIT WIDTH (kN/m)		
Specimen	Due to 77 Days of Cumulated Strain (XD/MD)	Max. Incremental Response to a Static Load (58 kN) (XD/MD)
PGG	2.4 / 0.1	0.4 / 0.4
KGG	1	0.2
WGT	2.9 / 1.8	0.6 / 0.2

The strain data results indicate that PGG and WGT sections absorb the most tensile stress at the bottom of the subbase. The results are somewhat unexpected when looking at the material strengths as presented in Table 1. The same strength is reported for both grids while the textile is reported to have about twice the strength. However, this brings to light the importance of geosynthetic engagement with the surrounding soil. Thus, apparent tensile force appears to be related to the stress/strain transfer that occurs at the interface of the geosynthetic. In this demonstration the geotextile, which has the greatest strength, shows a similar tensile force contribution compared to that of the

weaker GT section. These results indicate a possible effect likely caused by different stress/strain transfer for different geosynthetics.

The maximum incremental response results for the static load tests show similar patterns as compared to the cumulative results. Furthermore, elastic layer theory predicts similar results to those measured. Kenlayer software was used to perform an elastic analysis based on parameters measured and moduli determined by FWD results (Huang 1993).

Additionally, gage survivability has been better than expected with 87 and 83 percent still responding after approximately 3 and 7 months, respectively. Other researchers have indicated only 3 to 4 months of time prior to failure of the foil type strain gages (Al-Qadi et al. 1999).

4.2 FWD Results

Additional field tests performed in September, October, December and March that consisted of FWD observations were used to compare performance of the different demonstration test sections. Maximum deflections recorded during the FWD tests for 90-kN falling weight are presented in Figure 14. Maximum deflection, which is measured at the center of the loading plate, is a gross indicator of the aggregate pavement response to the dynamic load. Larger deflections were obtained in the spring for the sections. But, the smallest deflections were measured through the test sections in winter 1999. The maximum deflection from the test section ranged from 0.4 mm to 0.6 mm (Fall and Winter 1999), 2.1 mm to 2.6 mm (Spring 2000). Overall, the test sections

were essentially equivalent thus enabling support of construction equipment during the severest challenge to the soft subgrade in terms of stresses. Spring thaw-weakening is known to result in large decreases in pavement stiffness, e.g. 35 to 60 % compared to the normal conditions (Jong et al. 1998).

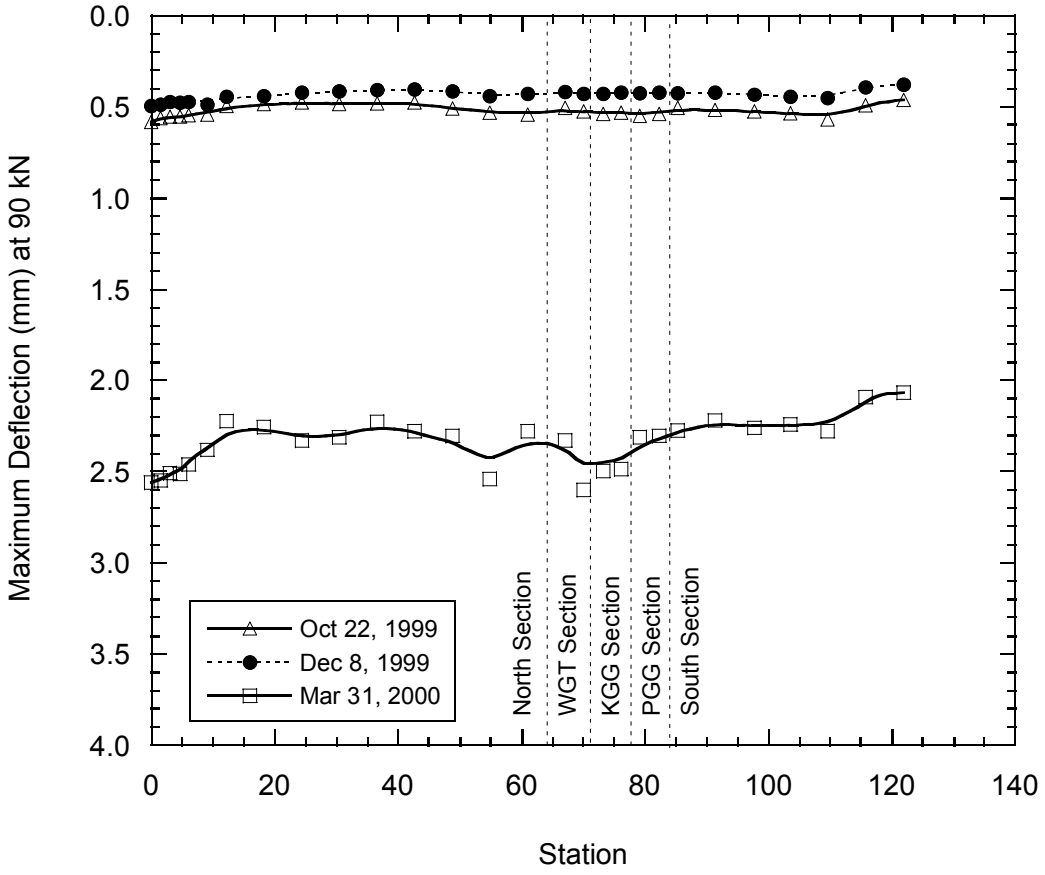

Figure 14. Maximum Deflection From Falling Weight Deflectometer Tests After Construction, Winter, and following Spring.

Deflection basins from the FWD survey data collected in each season are shown in Figure 15. Seasonal deflection basins showed that the basins are deeper and narrower in spring, which reflects the effect of

thaw-weakening. Greater deflections are typical during the spring due to warm and wet conditions that prevail. It can be expected that pavement stiffness recovers again in summer and the rest of the season.

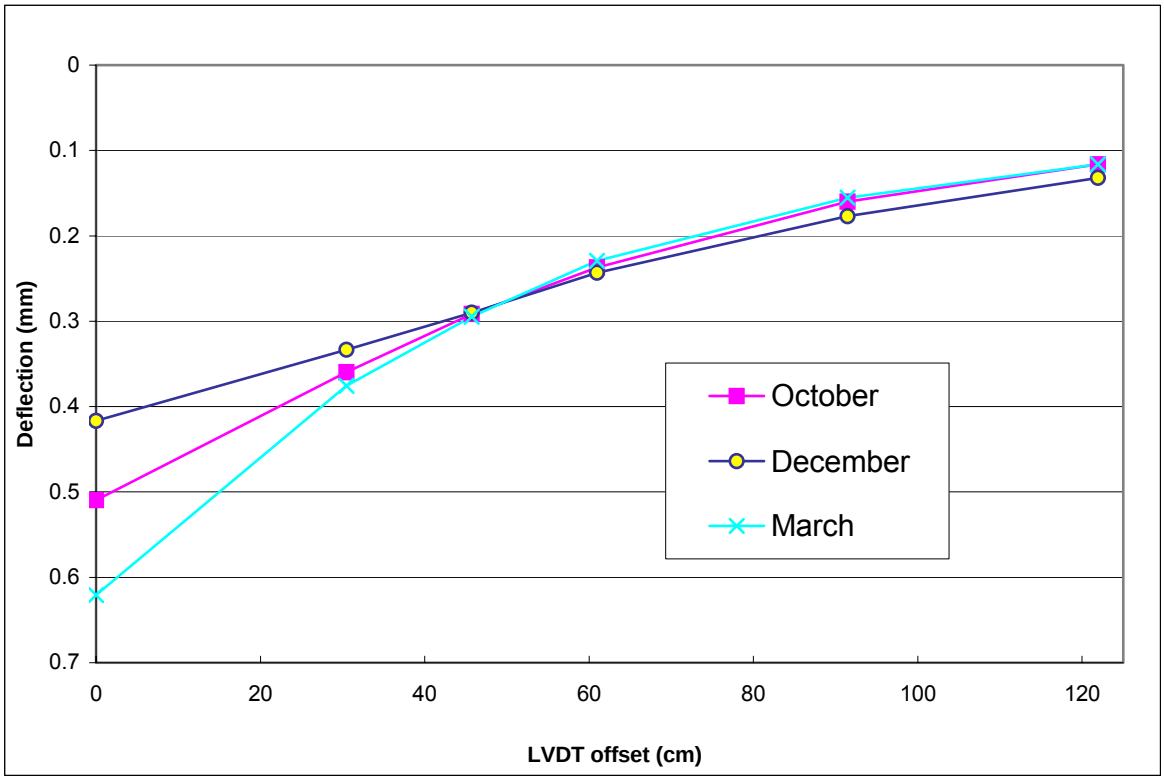

Figure 15. Seasonal Deflection Basins Showing Greater Deflection in the Spring.

Back-calculated modulus for each pavement layer across the tested alignment at USH 45 is shown in Figure 16. Figure 16 shows the back-calculated values for the subgrade modulus during the 3 different months from FWD data collected at the 40 kN load level. FWD test results indicate a subgrade modulus near 100 MPa. However, the moduli values across the test sections, which are underlain by different types of geosynthetic, vary little with no distinguishable pattern. Greater seasonal variability of the subgrade is also

noted that appears to be simply due to the properties of fine-grained subgrade soil. Also, recall that moduli, Poisson's ratios, layer thickness and depth to stiff layer were fixed at a typical value or directly measured for upper layers. Explanations of these are provided in Section 3.10. Similar relationships were found for the other three different load levels.

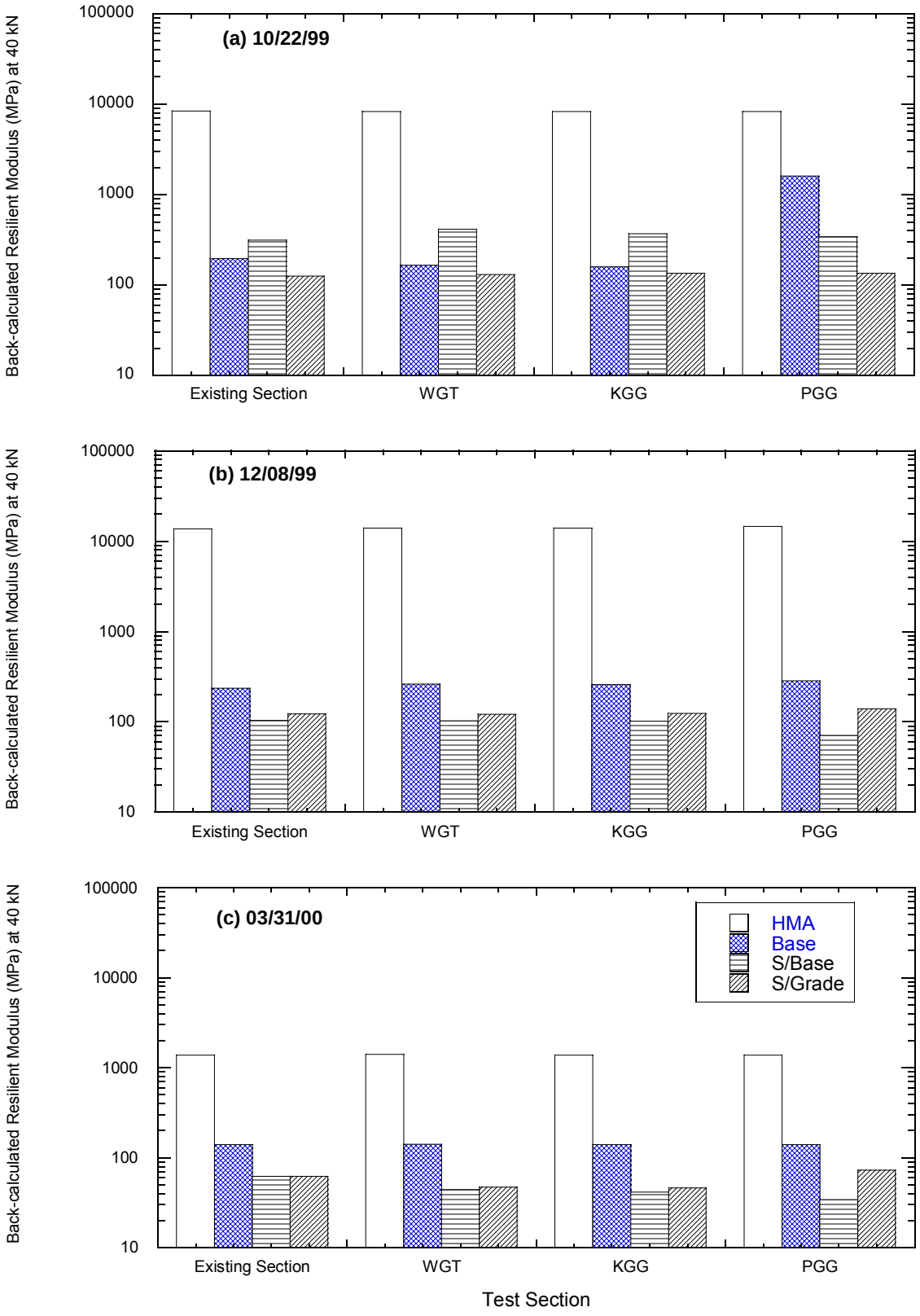

Figure 16. Back-calculated Modulus at 40 kN For Each Layer along USH 45 Test Sections.

5. ADDITIONAL INVESTIGATIONS

While much has been learned about instrumentation and FWD data analysis, this project was inconclusive with respect to the effectiveness of geosynthetics in stabilizing soft subgrade. USH 45 construction incorporated the geosynthetics but because a thick aggregate layer was used their overall effectiveness and differences from each other could not be discerned. Consequently, additional investigations involving both large-scale laboratory experiments and another field test site at STH 60 reconstruction project was undertaken. The results of this additional investigation are reported in "Equivalency of Crushed Rock with Industrial By-Products and Geosynthetic-Reinforced Aggregates Used for Working Platforms During Pavement Construction" (WHRP Project SPR #0092-00-12). A paper based on that report and pertaining to the geosynthetic-reinforced working platforms is given in Appendix A.

In the additional investigation, large-scale experiments were conducted on working platforms of crushed rock (breaker run stone or Grade 2 gravel) overlying a simulated soft subgrade. The tests were intended to simulate conditions during highway construction on soft subgrades where the working platform is used to limit total deflections due to repetitive loads applied by construction traffic. Tests were conducted with and without geosynthetic reinforcement to evaluate how the required thickness of the working platform is affected by the presence of reinforcement. Four different geosynthetics were used (geogrid, woven geotextile, nonwoven geotextile, and drainage composite),

each having different *in situ* extensibility. A geosynthetic-reinforced working platform was considered equivalent to a breaker run platform if the total deflection of the reinforced material was equal to that of the breaker run platform under the same construction loading.

Working platforms reinforced by geosynthetics accumulated deformation at a slower rate than unreinforced working platforms, and in most cases deformation of the geosynthetic-reinforced working platforms nearly ceased after 200 loading cycles. As a result, total deflections were always smaller (about a factor of two) for reinforced working platforms relative to unreinforced working platforms. Smaller deflections were also associated with working platforms that were thicker or reinforced with less extensible geosynthetics.

Thicknesses for equivalent working platforms reinforced with various types of geosynthetics were developed for a range of target total deflections and related to a measure of *in situ* extensibility characterized by an interaction modulus obtained from a pullout test. The equivalent thickness of geosynthetic reinforced material diminished approximately linearly with increasing logarithm of the interaction modulus (decreasing *in situ* extensibility of the geosynthetic). Moreover, the thickness ratio is lower when the target total deflection is smaller, indicating that the benefits of geosynthetic reinforcement are greater when the target deflection is lower.

The relationships in the equivalency table are based on the LSME tests for the specific geosynthetics used in this study and for a very soft subgrade condition. Therefore, the generality of the findings is not implied. However, this

methodology, including the interaction modulus, can be considered in other reinforcement-aggregate platforms.

6. CONCLUSIONS AND RECOMMENDATIONS

Much has been learned about instrumentation of geosynthetics with foil-type strain gages. First, installation procedures used during this demonstration project appear to be a success and are recommended for future projects. Weatherization techniques also appear to have been successful and are recommended to be utilized in future projects. Future geosynthetic strain gage applications need to be carefully planned well in advance, then appropriate modifications can be made during installation to satisfy the unique application. Additionally, better strain gage results are possible for a geotextile, based on Farrag's (1999) comments, when a longer (25 mm) strain gage is used to measure strain. Future installations are recommended to include a multiplexer and labview software so real time strain data can be collected and viewed at the same time.

On a more technical note, strain readings of geosynthetics were converted successfully into apparent tensile force contributions for geosynthetics placed in an actual highway application. Using these methods, strain data was collected successfully up to 7 months after field installation. Extreme care is needed during initial placement to avoid fatal damage of the strain gages and to insure the exact position of gages below the surface. However, it's important to note that for these applications the foil type strain gages all failed at approximately

four percent strain, based on laboratory results, due to loss of geosynthetic adherence. Different techniques are recommended when greater strains are expected. Although, Farrag (1999) does show that greater strains may be measured with longer gages when greater amounts of epoxy are utilized, however reinforcement effects of excess epoxy that are likely were not addressed.

The falling weight deflectometer does not provide sufficient resolution to differentiate between different types of geosynthetic test sections especially in a field environment where there's heterogeneity of natural soils. However, a control section without reinforcement was not constructed at this time that would have allowed for comparison and assessment of the geosynthetic addition. Perhaps, in a more controlled environment, deflection basin observations can be utilized for comparison of different types of geosynthetics where variable conditions can be limited. Additionally, WESDEF software, which is similar to MODULUS software, provided by the U.S. Army Corp of Engineers may be appropriate for further analysis of falling weight deflectometer data, as recommended by an author of the MODULUS software.

An additional investigation was conducted to delineate the effectiveness of geosynthetic reinforcement. According to this additional investigation, working platforms reinforced by geosynthetics accumulated deformation at a slower rate than unreinforced working platforms, and in most cases deformation of the geosynthetic-reinforced working platforms nearly ceased after 200 loading cycles. As a result, total deflections were always smaller (about a factor of two)

for reinforced working platforms relative to unreinforced working platforms. Smaller deflections were also associated with working platforms that were thicker or reinforced with less extensible geosynthetics.

REFERENCES

Al-Qadi, Imad L.; Bhutta, Salman A. (1999), "In Situ Measurements of Secondary Road Flexible Pavement Response to Vehicular Loading," Transportation Research Board, 1652, National Research Council, National Research Council, Washington, D.C., pgs. 206-216.

Austin, Deron N.; Wu, Kevin J.; White, David F.(1993) "The Influence of Test Parameters and Procedures on the Tensile Modulus of Stiff Geogrids," Geosynthetic Soil Reinforcement Testing Procedures, ASTM STP 1190; S.C. Jonathan Cheng, Ed.; American Society for Testing and Materials; Philadelphia, PA, pgs. 90-110.

Barenburg, E. J., Dowland, J. H., and Hales, J. H., "Evaluation of Soil Aggregate Systems with Mirafi Fabric," Civil Engineering Studies, Department of Civil Engineering, University of Illinois, August, 1975.

Barksdale, R. D., Brown, S. F., and Chan, F. Potential Benefits of Geosynthetics in Flexible Pavement Systems, Program Report 315, Transportation Research Board, National Research Council, November, 1989.

Bosscher P., Da-Tong J., Benson C.; "Software To Establish Seasonal Load Limits For Flexible Pavements," Cold Regions Impact On Civil Works, ASCE, Ninth International Conference on Cold Regions Engineering, Duluth, MN, 9/1998, 731-747.

Das, Braja M.; Khing, Kim H.; Shin, EunC.; "Stabilization of Weak Clay with Strong Sand and Geogrid at Sand-Clay Interface," Transportation Research Board, 1611, National Research Council, National Research Council, Washington, D.C. 1998, pgs. 55-62.

Farrag, Khalid, ; "Strain Gages Installation on Geosynthetics," 1999, Louisiana Transportation Research Center, 4101 Gourrier Avenue, Baton Rouge, LA 70808, 1-9.

Giroud, J.P. and Noiray, L. (1981) "Geotextile-Reinforced Unpaved Road Design," Proc. ASCE Journal Geotechnical Engineering, Vol. 107, No. GT9, 1233-54.

Giroud and Noiray, “Design of Unpaved Roads and Trafficked Areas with Geogrids.” Proceedings of Conf. Polymer Grid Reinforcement, Science and Engineering Research Council, London, March, 1984, pp 116-127.

Haas, Ralp; Walls, Jamie; Carroll, R.G.; “Geogrid Reinforcement of Granular Bases in Flexible Pavements,” Transportation Research Board, 1188, National Research Council, National Research Council, Washington, D.C. 1988, pp. 19-27.

Henry, Karen S.; “Geotextile Reinforcement of Low-Bearing-Capacity Soils (Comparison of Two Design Methods Applicable to Thawing Soils),” Special Report 99-7, June 1999, US Army Corps of Engineers, Cold Research & Engineering Laboratory.

Holtz, R. D., Christopher, B. R., and Berg, R. R., Geosynthetics Design and Construction Guidelines, Federal Highway Administration, US Dept. of Transportation, Washington, D.C., 1995.

Huang, Yang H., Pavement Analysis and Design, Virginia Dunn, Editor, 1993, Prentice Hall, Englewood Cliffs, New Jersey 07632.

Jones, C.J.F.P.; ”The Development and Use of Polymeric Reinforcements in Reinforced Soil,”The Practice of Soil Reinforcing in Europe, Ingold, T.S., Editor, 1995, Thomas Telford Services Ltd, Thomas Telford House, 1 Heron Quay, London, E144JD, pgs. 1-32.

Jong, D., Bosscher, P., and C. Benson. “Field Assessment of Changes in Pavement Moduli Caused by Freezing and Thawing,” Transportation Research Record 1615, TRB, national Research Council, Washington, D.C., 1998, pp. 41-50.

Strategic Highway Research Program (SHRP), “Field validation of SHRP asphalt binder and mixture specification tests,” 1993, Roque, R., Hilunen, D., Stoffels, S., Association of Asphalt Paving Technologists, St. Paul, MN, Vol. 62, 615-638.

Steward, J., Williamson, R., and Mohney, J., Guidelines for Use of Fabrics in Construction and Maintenance of Low-Volume Roads, USDA, Forest Service, Portland, OR, 1977.

Tensar Technical Note, July 1998, Tensa Earth Technologies, Inc. 5775B Glenridge Drive, Suite 450, Atlanta, GA 30328.

APPENDIX A

DEFLECTION OF PROTOTYPE GEOSYNTHETIC-REINFORCED WORKING PLATFORMS OVER SOFT SUBGRADE

PAPER NO 06-2285

TITLE:

DEFLECTION OF PROTOTYPE GEOSYNTHETIC-REINFORCED WORKING PLATFORMS OVER SOFT SUBGRADE

Author(s):

1. Woon-Hyung Kim

Managing Director, Geotechnical Department, Dasan Consultant Co. Seoul, Republic of Korea
(Former Graduate Assistant, Dept. of Civil and Environmental Engineering, University of Wisconsin-Madison, Madison, WI 53706, USA)
Tel: 011-82-2-2222-4389 Fax: 011-82-02-539-1115 e-mail: whkim@dasan93.co.kr

2. Tuncer B. Edil (Corresponding Author)

Professor, Dept. of Civil and Environmental Engineering, University of Wisconsin-Madison, Madison, WI 53706, USA.
Tel: (608) 262-3225 Fax: (608) 263-2453 e-mail: edil@engr.wisc.edu

3. Craig H. Benson

Professor, Dept. of Civil and Environmental Engineering, University of Wisconsin-Madison, Madison, WI 53706, USA.
Tel: (608) 262-7242 Fax: (608) 263-2453 e-mail: benson@engr.wisc.ede

4. Burak F. Tanyu

Engineer, GeoSyntec Consultants, Chicago Branch
55 W Wacker Dr., Suite 1100, Chicago, IL, 60601.
Tel: (312) 658-0500 Fax: (312) 658-0576 e-mail: btanyu@geosyntec.com

Paper submitted for publication at

Transportation Research Record

2006 Annual Meeting

Abstract: Large-scale experiments were conducted on working platforms of crushed rock (breaker run stone or Grade 2 gravel) overlying a simulated soft subgrade to mimic conditions during highway construction where a working platform is used to limit total deflections due to construction traffic. Tests were conducted with and without geosynthetic reinforcement to evaluate how deflection of the working platform is affected by the presence of reinforcement, type of reinforcement, and thickness of the working platform. Four different geosynthetics were used (geogrid, woven geotextile, nonwoven geotextile, and drainage composite). Reinforced working platforms deformed at a slower rate, and in most cases deformation of geosynthetic-reinforced working platforms nearly ceased after ≈ 200 loading cycles. Total deflections at 1000 cycles were about a factor of two smaller for reinforced working platforms relative to unreinforced working platforms, and smaller deflections were associated when less extensible geosynthetics were used for reinforcement. The thickness of a geosynthetic reinforced working platform needed to meet a target deflection diminished approximately linearly with increasing logarithm of the interaction modulus, a measure of *in situ* extensibility measured in a pull-out box. The reduction in working platform thickness attained with reinforcement was also larger when the target total deflection was smaller.

Key Words: working platform, geosynthetic reinforcement, large-scale model experiment, soft subgrade, interaction modulus, pull-out test.

INTRODUCTION

Construction on soft subgrade soils has been identified as a major issue affecting cost and scheduling of highway projects in regions where soft subgrades are common (*1*). To facilitate construction, typically a working platform is constructed by undercutting the soft subgrade and replacing it with a layer of "select" granular material that can support heavy wheel loads applied by construction traffic (*2*). In Wisconsin, USA, this select material is crushed rock referred to as 'breaker run' stone. The intent of the working platform is to maintain the total deflection under a typical construction wheel load below a level considered acceptable for placement of overlying pavement layers. Recent studies indicate that acceptable total deflections in Wisconsin range between 25 and 50 mm (*3*).

Working platforms constructed with granular materials generally have been effective in Wisconsin (*4*). However, they are costly to construct, particularly as the haul distance from the source of granular material increases. Consequently, transportation agencies such as the Wisconsin Department of Transportation (WisDOT) are seeking methods to reduce the costs associated with working platforms (*4*). One method under consideration is to reduce the required thickness of the working platform by reinforcing the granular material with geosynthetics. For example, Leng and Gabr (*5*) showed that geogrid reinforcement of a granular layer reduced surface deformations by 20 to 30% under wheel loads. This application is analogous to aggregate reinforcement in unpaved roads (*5-9*), except working platforms for pavement construction over soft subgrade are subjected to fewer cycles of higher intensity loads requiring lower acceptable total deflections to allow pavement construction. To keep construction costs low and to expedite construction, the practice in Wisconsin is to place the reinforcing geosynthetic at the interface between the soft subgrade and the granular layer.

The reduction in deflection under wheel loads that is achieved by placing a geosynthetic layer between the subgrade and granular layer has been attributed to several factors. One factor is the reduced likelihood of local bearing capacity failure of the subgrade due to concentrated wheel loads provided by the geosynthetic membrane effect (*9, 10*). Another is the reduction in stress on the subgrade due to greater stress distribution in the granular layer (*9,11,*

12). Membrane-type of support of the granular layer where deep rutting occurs as described in Giroud and Noiray (*7*), Giroud et al. (*8*), and Giroud and Han (*9*), and changing the magnitude and orientation of shear stresses on the subgrade in the loaded area (*9*) may also be important. Restricting lateral movement of the base course material and the subgrade soil is also considered to contribute to reduced deflections (*9, 13*). It is noted that there is a significant difference between geogrids and other types of geosynthetics such as geotextiles in terms of reinforcement because geogrids interlock with the aggregate whereas other geosynthetics do not (*9*).

The objective of this study was to evaluate the total deflection of granular working platforms reinforced with four geosynthetic materials under repetitive loads typical of construction traffic, and to relate the total deflections to the relative extensibility of the geosynthetics. The study was directed to respond to needs in Wisconsin, but the findings are applicable to other locations where working platforms are constructed on soft subgrades with crushed rock. Geosynthetic-reinforced working platforms were considered "equivalent" to thicker unreinforced working platforms if the reinforced platforms deflected an equal or lesser amount under typical construction loading than the unreinforced working platforms. Other factors may also be important when defining equivalency in the context of pavement performance, such as drainage and long-term durability. These factors should be considered by the designer, but were not within the scope of this study.

MATERIALS

Soils

Two granular materials were used in this study: Grade 2 gravel and breaker run stone. Grade 2 gravel is commonly used as base course in Wisconsin and consists of crushed rock screened to the WisDOT gradation criteria shown in Fig. 1. According to WisDOT (*2*), breaker run stone is a broadly graded "large-sized aggregate resulting from crushing of rock, boulders, or large stone that is not screened or processed after initial crushing." Breaker run stone typically has much larger particles and is more broadly graded than Grade 2 gravel.

The breaker run rock and Grade 2 gravel used in this study were retrieved during re-construction of a portion of Wisconsin State Trunk Highway 60. Both are derived from Cambrian dolostone in southern Wisconsin (*14*). Particle size characteristics and other physical properties of the materials are summarized in Table 1; the particle size distribution curves are shown in Fig. 1. Both materials are coarse grained and classify as well-graded gravel (breaker run) and well-graded sand (Grade 2 gravel) in the Unified Soil Classification System (USCS). Despite the classification of Grade 2 gravel as sand, the gravel nomenclature is retained herein because of its common usage in Wisconsin. Compaction tests indicated that the Grade 2 gravel is nearly insensitive to compaction water content due to low fines content (8%) (*15*). A compaction test could not be conducted on the breaker run stone because of its large particle size. However, breaker run stone contains only a small amount of fines (3%), and thus is also believed to be insensitive to compaction water content.

Geosynthetics

Four different geosynthetics were used in this study: (i) a biaxial polypropylene geogrid, (ii) a polypropylene slit-film woven geotextile, (iii) a polypropylene nonwoven needle-punched geotextile, and (iv) a drainage geocomposite consisting of a tri-planar polyethylene geonet (triangular-shaped mesh structure with three sets of overlaid strands) with nonwoven polypropylene geotextiles heat bonded to each side. Basic characteristics and mechanical properties of the geosynthetics are summarized in Table 2. The geogrid and woven geotextile are conventional reinforcing geosynthetics. The nonwoven geotextile is used for separation, but was evaluated in this study to assess whether appreciable reinforcement could also be realized.

Similarly, drainage geocomposites are used primarily for drainage and separation, but they may also provide reinforcement.

Relative extensibility of the geosynthetics alone (not in soil) was characterized using wide-width tensile tests conducted in accordance with ASTM D 4595. Relative extensibility of the geosynthetics buried in soil (referred to as *in situ* extensibility herein) was characterized using pull-out tests conducted in accordance with Geosynthetic Research Institute (GRI) GG6 (geogrid) or GT6 (geotextiles and drainage composite). The pull-out box described by Tatlisoz et al. (*16*) and Goodhue et al. (*17*) was used for the pull-out tests. Force-elongation curves from the wide-width tensile tests are shown in Fig. 2. Curves relating pull-out force to displacement at various points on the geosynthetic are shown in Fig. 3. All of the geosynthetics failed in tension during the pullout tests.

For the pull-out tests, the geosynthetics (1.31 m x 0.41 m) were embedded in Grade 2 gravel (90 mm below, 300 mm above) compacted to 95% of maximum density per standard Proctor test. A normal stress of 6.3 kPa was applied (corresponding to a 0.30-m thick working platform of Grade 2 gravel layer above the geosynthetic) and pull-out was conducted at 1 mm/min, with the pull-out load measured using a load cell mounted on the head. Displacements along the geosynthetic (0, 80, 220, and 420 mm from the front) were measured with linear variable differential transformers (LVDTs) attached to steel telltale wires encased in polyethylene tubing as described in Tatlisoz et al. (*16*).

Without soil interaction (i.e., wide-width tensile tests), the drainage composite and woven geotextile are the least extensible of the geosynthetics tested, the nonwoven geotextile is the most extensible, and the geogrid has intermediate extensibility (Fig. 2). The drainage geocomposite also has the largest tensile strength (52 kN/m in the machine direction, MD) and the geogrid and nonwoven geotextile the lowest tensile strength (18 and 14 kN/M in MD) (Fig. 2, Table 2). When embedded in the Grade 2 gravel (pull-out tests), however, the geogrid and woven geotextile are less extensible and the nonwoven geotextile and drainage geocomposite are more extensible (Fig. 3). For example, at a pull-out load of 10 kN/m, displacement at the front of the geosynthetic was 6 mm for the nonwoven geotextile, 8 mm for the geogrid, 15 mm for the drainage geocomposite, and 66 mm for the nonwoven geotextile (Fig. 3).

An interaction modulus (M_i) was computed for each of the geosynthetics using the pull-out data:

$$M_i = \frac{F_p / W L_g}{\Delta_f / L_g} \tag{1}$$

where F_p is the maximum pullout force, W is the width of the geosynthetic, L_g is the total length of the geosynthetic in the pullout test, and Δ_f is the front displacement of the geosynthetic corresponding to F_p. The modulus M_i is an index of the *in situ* extensibility of the geosynthetics and reflective of the degree of engagement between a geosynthetic and granular material. Other descriptions of this interaction could have been used (e.g., the nonlinear interface shear stress-shear displacement relationship in Madhav et al. (*18*) or Perkins and Cuelho (*19*). However, a simple index of interface interaction based on directly measured quantities was preferred in this study. A summary of the M_i is in Table 2. The M_i ranges from 699 kPa (geogrid) to 77 kPa (nonwoven geotextile), indicating that the geogrid is the least extensible and the nonwoven geotextile the most extensible when embedded in Grade 2 gravel.

LARGE-SCALE MODEL EXPERIMENT (LSME)

Deflection of working platforms incorporating geosynthetic reinforcement was evaluated in an apparatus referred to as the large-scale model experiment (LSME) that is used for evaluating pavement deflections during cyclic loading in a manner that replicates field conditions as closely

as practical (*15*). The LSME consists of a loading system and a prototype-scale pavement structure (or parts of it) constructed in a 3 m x 3 m x 3 m test pit. A schematic of the LSME is shown in Fig. 4. A detailed description of the apparatus can be found in Tanyu et al. (*15*).

Subgrade and Pavement Profile

The subgrade and pavement profile tested in this study consisted of five layers (from bottom to top): (i) dense uniform sand (2.5 m) simulating a stiffer underlying layer, (ii) 0.45 m of expanded polystyrene (EPS) geofoam simulating soft subgrade, (iii) 0.025 m of Grade 2 gravel, (iv) a geosynthetic layer, and (v) a layer of granular material (Grade 2 gravel or Breaker run) simulating a working platform. Base course and asphalt were not included in the profile because the objective was to evaluate deflection of the working platform layer under construction traffic loads. The thin (0.025 m) layer of Grade 2 gravel placed over the EPS (Fig. 4) was used to facilitate interaction with the geosynthetic (i.e., an interface obtained by placing the geosynthetic directly against the EPS was not considered realistic).

The EPS layer was used in lieu of earthen subgrade materials to facilitate replication of experiments. A series of tests was conducted on a variety of EPS materials to identify an EPS with similar stress-strain behavior as a typical soft subgrade soil in Wisconsin. Details of this testing program are beyond the scope of this paper, but can be found in Tanyu et al. (*15*). The EPS that was selected has a modulus similar to that of soft-subgrade soils found in Wisconsin (7 MPa or lower) under the loads applied to the subgrade layer in the LSME (< 100 kPa) (*15*). Negussey and Jahanandish (*20*) also report that the stress-strain behavior of low-density EPS (21.0 kg/m^3) is comparable to that of soft inorganic clays of moderate plasticity. The EPS underwent plastic deformation, as occurs in a conventional subgrade soil in response to long-term repetitive loading, and some embedment of gravel into the EPS occurred.

Working platforms 0.30-m- and 0.46-m-thick comprised of breaker run or Grade 2 gravel were placed on top of the geosynthetics. Additional thicknesses were not evaluated due to the high level of effort associated with setting up the LSME. Working platform materials were placed in lifts 0.08- to 0.11-m thick and were compacted with a vibratory plate compactor. Each lift was compacted until the dry unit weight exceeded 95% of maximum dry unit weight (Grade 2 gravel) or 20.0 kN/m^3 (breaker run stone). A nuclear density gage was used to monitor the dry unit weight during compaction. Because of their insensitivity to water content during compaction, the Grade 2 gravel and breaker run stone were placed in the LSME at their existing water content (≈ 5%).

Loads and Deflections

All of the pavement profiles in the LSME were subjected to loads of high intensity and short duration simulating heavy truck traffic directly on the working platform during construction. The construction loads were selected to simulate the load applied by loaded 4-axle dump trucks (70 kN per axle, and 35 kN per wheel set). These trucks normally have a tire pressure of approximately 700 kPa, which results in a contact area of 0.05 m^2 under a 35 kN load.

The 35-kN load was applied with a MTS hydraulic actuator attached to a 25-mm-thick circular steel plate having a diameter of 250 mm (area = 0.05 m^2) (Fig. 4). A haversine load pulse was applied that consisted a 0.1-s load period followed by a 0.9-s rest period. The same load pulse is used in the laboratory resilient modulus test (AASHTO T294). One thousand load cycles were applied to simulate the typical level of construction traffic applied to a working platform in Wisconsin (*21*).

Vertical deflections of the pavement profile were measured directly beneath the loading plate and at radial distances of 300, 450, and 650 mm. Position transducers anchored to the surface of the working platform were used to measure surface deflections outside the footprint of the loading plate (*15*). Replicate measurements were made at distances of 300 and 450 mm on opposite sides of the loading plate. These replicate measurements generally differed by less

than 10% at a given distance, and thus the average of these deflections was recorded. All of the load and deflection data were recorded by a CR9000 datalogger manufactured by Campbell Scientific Inc.

Geosynthetic Movements and Strains

Movement of the geosynthetics was measured using LVDTs attached to steel telltale wires anchored to the geosynthetic in the cross machine direction at radial distances of 0, 130, 255, and 510 mm from the center of the loading plate. The telltales were encased in polyethylene tubing. Strains in the geosynthetic were measured with resistance-type strain gages (Micro-Measurement EP-08-250BG-120 for geogrid and drainage geocomposite, EP-08-20CBW-120 for geotextiles, Vishay Intertechnology, Malvern, PA) attached on the upper and lower surfaces of the geosynthetic in the cross-machine direction at five different radial distances from the center of the loading plate: 0, 130, 255, 380, and 510 mm. A detailed description of the methods used to install and calibrate the telltales and strain gages can be found in Kim (*22*).

Methods described in Chew et al. (*23*) were used to attach strain gages to the geotextiles. Each strain gage was mounted on a thin plastic strip and the strip was attached to the surface of the geotextile using two aluminum end plates with an adhesive. This method prevents local stiffening (geotextile or gage) that can occur when epoxy adhesives are used for attaching strain gages. Methods described in Hayden et al. (*24*) were used to attach strain gages to the geogrid and the drainage geocomposite. Ribs in both of these geosynthetic materials are too narrow for direct mounting of strain gages. Thus, strain gages were mounted on polyethylene dog-bones, and the dog bones were used in place of ribs in the geogrid or drainage geocomposite core (geonet). The dog bones were sized to provide equivalent cross-section as the ribs that were replaced, and were attached to adjacent ribs using bolted clamps. All strain gauges were calibrated in wide-width (200 mm) tensile tests using extensometers.

RESULTS AND ANALYSIS

Accumulation of Centerline Deflection

Cumulative total deflections (δ_t) under the loading plate of the LSME are shown in Fig. 5 as a function of the number of load cycles for working platforms having a thickness (h) of 0.30 m or 0.46 m. Total deflection accumulates monotonically during the LSME tests for all of the working platforms, with the greatest rate of accumulation during the first 100 cycles. Subsequently, the deformation rate decreases as the number of load cycles increases until a steady-state condition is reached (≈ 200 load cycles). This steady-state condition is either a nearly constant rate of accumulation or near complete cessation of the accumulation.

The effect of the geosynthetic reinforcement is evident in Fig. 5. In all cases, δ_t is lower at 1000 cycles when the working platform includes geosynthetic reinforcement regardless of whether the working platform is 0.30 or 0.46 m thick (18%-40% lower for the 0.30-m-thick working platforms, 31%-51% for the 0.46-m-thick platforms). Also, in most cases, the rate of accumulation is lower (or ceases) beyond 200 cycles when the working platform includes geosynthetic reinforcement (the 0.30-m-thick working platform reinforced with the nonwoven geotextile is an exception). In contrast, for three of the four unreinforced working platforms, the rate of accumulation increases continuously throughout the test (the test with 0.46-m of breaker run is the exception).

Total Deflection Basins

Deflection basins (total deflection vs. radial distance from the center of the loading plate) during the 1000th loading cycle are shown in Fig. 6. In all cases, the deflections are largest directly under the loading plate, and are essentially the same at the center (0 mm) and edge of the

loading plate (300 mm). The deflections also diminish rapidly with distance from the edge of the loading plate (> 300 mm), and vary only a small amount for radial distances ≥ 400 mm. Consequently, the remaining discussion focuses primarily on deflections directly underneath the loading plate.

The effect of thickness of the working platform on the total deflection basin is illustrated in Fig. 6a using data from working platforms of Grade 2 gravel either unreinforced (left panel) or reinforced with the geogrid or the nonwoven geotextile (right panel). Thicker working platforms have shallower deflection basins due to the additional stress distribution and corresponding reduction in strain in a thicker layer (*15*), regardless of the presence of reinforcement or the type of reinforcement used. For example, increasing the thickness of the unreinforced working platform from 0.30 m to 0.46 m results in a reduction in centerline deflection of 43%. Similarly, increasing the thickness of a reinforced working platform from 0.30 m to 0.46 m decreases the center deflection by 53% with the more extensible nonwoven geotextile or 54% with the less extensible geogrid.

Comparison of the deflection basins in Fig. 6a also shows that deflections of thinner reinforced working platform can be comparable to those for a thicker unreinforced working platform. For example, the centerline deflection is essentially the same for a 0.30-m-thick working platform reinforced with geogrid and a 0.46-m-thick unreinforced working platform. That is, a thinner working platform with equivalent total deflection can be achieved by reinforcing the granular material.

The effect geosynthetic type is shown Fig 6b using data for a 0.30-m-thick working platform of Grade 2 gravel either unreinforced (left panel) or reinforced with one of the four geosynthetics (right panel). A shallower deflection basin is obtained when the working platform is reinforced with geosynthetics, regardless of the type of reinforcement used, and the depth of the deflection basin is related inversely to the interaction modulus (Table 2). That is, geosynthetics with a higher interaction modulus (M_i) have shallower deflection basins. For example, deflection under the loading plate is 23 mm for the geogrid (M_i = 699 kPa) and 31 mm for the nonwoven geotextile (M_i = 74 kPa). Thus, incorporating geosynthetic reinforcement makes a working platform stiffer under cyclic loads, with greater stiffness being obtained with less extensible geosynthetics.

Correspondence does not exist between depth of the deflection basin and the relative extensibilities observed in the wide-width tensile tests (Table 2). For example, the offset tangent modulus is 88.3 kN/m for the geogrid and 675 kN/m for the drainage composite, whereas the deflection basin is deeper for the drainage composite than for the geogrid. This lack of correspondence reflects the absence of interaction and engagement with the soil during the wide-width tensile test. For example, deformation of a geogrid in soil is affected by friction on the rib surfaces and particles protruding through the apertures that bear on the ribs, neither of which is accounted for in the wide-width tensile test.

Geosynthetic Strain and Displacement

Strain and displacement of the geosynthetics at the edge of the loading plate are shown in Fig. 7. Strain and displacement at other points was negligible, indicating that most of the geosynthetic deformation occurred at the edge of the loading plate (*22*). In Fig. 7a, strain and displacement are shown for the geogrid and nonwoven geotextile in working platforms 0.30-m and 0.46-m thick. The geogrid and nonwoven geotextile were selected for Fig. 7a to represent the range of *in situ* extensibility of the four geosynthetics included in the study. Strain and displacement are shown in Fig. 7b for all four geosynthetics in working platforms 0.30-m thick. Positive telltale displacement refers to an inward movement of the geosynthetic and positive gauge strain refers to tension in the geosynthetic.

The effect of thickness is evident in the strain and movement in the geogrid at the edge of loading plate (300 mm) as a function of number of loading cycles (Fig. 7a). Less strain

and smaller movements occur when the working platform is thicker because the total deflections are smaller. In contrast, thickness has no noticeable effect on strain or displacement in the more extensible nonwoven geotextile. The effect of type of geosynthetic is shown in Fig. 7b. Greater strains occur in the less extensible geosynthetics, probably due to greater distribution of stresses.

This difference in deformation behavior between the geosynthetics may reflect greater strain distribution in the less extensible geosynthetics (geogrid and woven geotextile) than the more extensible materials (non-woven geotextile, drainage geocomposite). Strains and deformations must have occurred in each of the geosynthetic materials, because deformation of the soil occurred adjacent to the loading plate in the test pit. However, deformations in the more extensible geosynthetics may have localized between the points at which strain and displacements were measured, and therefore not detected by the strain gages and telltales.

PRACTICAL IMPLICATIONS

Working platform thicknesses required to maintain the cumulative total deflection during construction (assumed to be 1000 load cycles) below target maximum deflections (i.e., 12, 25, or 38 mm) were estimated from the LSME data (Fig. 5) for each type of working platform (breaker run stone, Grade 2 gravel, Grade 2 gravel with geosynthetic reinforcement). Because only two thicknesses were evaluated in the LSME (0.30 and 0.46 m), estimates of required thickness were made by linear interpolation between known combinations of working platform thickness and the total deflection at 1000 cycles. These estimates, reported in Table 3, are an approximation because the relationship between thickness and total deflection is not necessarily linear (*25*). However, the level of effort required to conduct tests at different thicknesses so as to define non-linearities was beyond the scope of the study. The reader should keep this limitation in mind when interpreting the results reported in Table 3.

Thicknesses required to meet the target maximum deflections are compared in Fig. 8 in terms of the thickness ratio (h/h_{br}), defined as the thickness required to achieve the target deflection for a given type of working platform (h) divided by the thickness required to achieve the same target deflection for a working platform of breaker run stone (h_{br}). The thickness ratio is greater than 1.0 (1.1-1.2) for all working platforms constructed with Grade 2 gravel without geosynthetic reinforcement because breaker run stone is stiffer than Grade 2 gravel, all other factors being equal (*25*). In contrast, when reinforcement is added to a working platform constructed with Grade 2 gravel, the thickness ratio is always less than 1.0, with smaller thickness ratios generally corresponding to geosynthetics with lower *in situ* extensibility. For example, when the target deflection is 25 mm, the thickness ratio is 0.78 for a working platform reinforced with the geogrid and 0.97 for a working platform reinforced with the non-woven geotextile. The thickness ratio also diminishes as the target total deflection decreases. Thus, geosynthetic reinforcement is more advantageous in applications where smaller total deflection is required.

The effect of relative *in situ* extensibility of the geosynthetics is shown in Fig. 9, which relates thickness ratio to the interaction modulus for total deflections of 25 mm and 38 mm. As the *in situ* extensibility decreases (interaction modulus increases), the thickness ratio diminishes (a thinner working platform is required to result in the same total deflection). Moreover, the thickness ratio is lower when the required total deflection is smaller, further illustrating that the benefits of geosynthetic reinforcement are greater when the required total deflection is lower.

It is noted that comparison of the plastic deformations obtained for the 0.3-m thick unreinforced breaker run and Grade 2 gravel platforms and Grade 2 gravel platform reinforced with the woven and nonwoven geotextiles with the rut depths estimated from the equations given by Giroud and Han (*26*) agreed well for an assumed subgrade CBR of 1.5 and 1000 loading cycles. Since an EPS layer was used to simulate the soft subgrade, its equivalent CBR is not precisely known. In the comparisons, the actual modulus ratio of the aggregate layer to

the subgrade in the experiments was used rather than the limiting value of 5 suggested by Giroud and Han (*26*).

SUMMARY AND CONCLUSIONS

Large-scale experiments were conducted on working platforms of crushed rock (breaker run stone or Grade 2 gravel) overlying a simulated soft subgrade. The tests were intended to simulate conditions during highway construction on soft subgrades where the working platform is used to limit total deflections due to repetitive loads applied by construction traffic. Tests were conducted with and without geosynthetic reinforcement to evaluate how the required thickness of the working platform is affected by the presence of reinforcement. Four different geosynthetics were used (geogrid, woven geotextile, nonwoven geotextile, and drainage composite), each having different *in situ* extensibility. A geosynthetic-reinforced working platform was considered equivalent to a breaker run platform if the total deflection of the reinforced material was equal to that of the breaker run platform under the same construction loading.

Working platforms reinforced by geosynthetics accumulated deformation at a slower rate than unreinforced working platforms, and in most cases deformation of the geosynthetic-reinforced working platforms nearly ceased after 200 loading cycles. As a result, total deflections were always smaller (about a factor of two) for reinforced working platforms relative to unreinforced working platforms. Smaller deflections were also associated with working platforms that were thicker or reinforced with less extensible geosynthetics.

Thicknesses for equivalent working platforms reinforced with various types of geosynthetics were developed for a range of target total deflections and related to a measure of *in situ* extensibility characterized by an interaction modulus obtained from a pullout test. The equivalent thickness of geosynthetic reinforced material diminished approximately linearly with increasing logarithm of the interaction modulus (decreasing *in situ* extensibility of the geosynthetic). Moreover, the thickness ratio is lower when the target total deflection is smaller, indicating that the benefits of geosynthetic reinforcement are greater when the target deflection is lower.

The relationships in the equivalency table are based on the LSME tests for the specific geosynthetics used in this study and for a very soft subgrade condition. Therefore, the generality of the findings is not implied. However, this methodology, including the interaction modulus, can be considered in other reinforcement-aggregate platforms.

ACKNOWLEDGEMENT

Financial support for this study was provided by the Wisconsin Department of Transportation (WisDOT) through the Wisconsin Highway Research Program (WHRP). Amoco Fabrics and Fibers Co., Tenax Corporation, and Yahara Materials donated materials used in the project. Tests in the LSME were conducted in the Structures and Materials Testing Laboratory (SMTL) at the University of Wisconsin-Madison. The conclusions and recommendations in this report are solely those of the authors, and do not necessarily reflect the opinions or policies of the sponsors or others who provided assistance during the study. Endorsement by persons other than the authors is not implied and should not be assumed.

REFERENCES

1. WisDOT, 1997, *Subgrade Design/Construction Process Review*, District 1 Final Report, State of Wisconsin, Department of Transportation.

2. WisDOT, 1996, *Standard Specifications for Highway and Structure Construction*, Wisconsin Department of Transportation, Madison, Wisconsin. p. 754.

3. Crovetti, J. A., and Schabelski, J. P., 2001, *Comprehensive Subgrade Deflection Acceptance Criteria*, Phase III Final Report WI/SPR 02-01, WisDOT, Highway Research Study #98-1, SPR #0092-45-95.

4. Edil, T. B., Benson, C. H., Bin-Shafique, M. S., Tanyu, B. F., Kim, W. H., and Senol, A., 2002, Field Evaluation of Construction Alternatives for Roadway Over Soft Subgrade, *Transportation Research Record*, 1786, Transportation Research Board, National Research Council, Washington, DC, pp. 36-48.

5. Leng, J., and Garb, M. A., 2002, "Characteristics of Geogrid-Reinforced Aggregate Under Cyclic Load," *Transportation Research Record 1786*, Transportation Research Board, National Research Council, Washington, DC, pp. 29-35.

6. Fannin, R. J., and Sigurdsson, O., 1996, "Field Observations on Stabilization of Unpaved Roads with Geosynthetics," *Journal of Geotechnical Engineering*, ASCE, Vo. 122, No. 7, pp. 544-553.

7. Giroud, J. P. and Noiray, L., 1981, "Geotextile Reinforced Unpaved Road Design," *Journal of Geotechnical Engineering Division*, ASCE, Vol. 107, No. GT9, pp. 1233-1254.

8. Giroud, J. P., Ah-Line, C., and Bonaparte, R, 1984, "Design of Unpaved Roads and Trafficked Areas with Geogrids," Polymer Grid Reinforcement: A Conference Sponsored by SERC and Netlon, Ltd., Thomas Telford, London, England, pp. 116-127.

9. Giroud, J. P. and Han, J., 2004a, "Design Method for Geogrid-Reinforced Unpaved Roads. I. Calibration and Applications," *Journal of Geotechnical Engineering Division*, ASCE, Vol. 130, No. 8, pp. 787-797.

10. Holtz, R. D., Christopher, B. R., and Berg, R. R., 1997, *Geosynthetic Engineering*, BiTech Publishers, Ltd., Richmond, B.C., Canada.,

11. Holtz, R. D., Christopher, B. R., and Berg, R. R., 1995, "Geosynthetic Design and Construction Guidelines," Report No. FHWA-HI-95, U.S. Department of Transportation, Federal Highway Administration, National Highway Institute Course No. 13213, Washington, DC.

12. Perkins, S. W., 1999, "Mechanical Response of Geosynthetic-Reinforced Flexible Pavements," *Geosynthetics International*, Vol. 6, No. 5, pp. 347-382.

13. Geosynthetic Materials Association, 2000, *Geosynthetic Reinforcement of the Aggregate Base/Subbase Courses of Pavement Structures*, GMA White Paper II, prepared for AASHTO Committee 4E.

14. Mudrey, M. G., Brown, B. A., and Greenberg, J. K., 1982, Bedrock Geologic Map of Wisconsin, Geological and Natural History Survey, University of Wisconsin-Extension.

15. Tanyu, B. F., Kim, W. H., Edil, T. B., and Benson, C. H., 2003, "Comparison of Laboratory Resilient Modulus with Back-Calculated Elastic Moduli from Large-Scale

Model Experiments and FWD Tests on Granular Materials," *Resilient Modulus Testing for Pavement Components, ASTM STP 1437*, Paper ID 10911, G. N. Durham, A. W. Marr, and W. L. De Groff, Eds., ASTM International, West Conshohocken, PA, 191-208.

16. Tatlisoz, N., Edil, T. B., and Benson, C. H., 1998, "Interaction Between Reinforcing Geosynthetics and Soil-Tire Chip Mixtures," *J. of Geotechnical and Geoenvironmental Engineering*, ASCE, 124(11), 1109 - 1119.

17. Goodhue, M., Edil, T. B., and Benson, C. H., 2001, "Interaction Between Reinforcing Geosynthetics and Foundry Sands," *Journal of Geotechnical and Geoenvironmental Engineering,*" American Society of Civil Engineers, Vol. 127, No. 4, pp. 353-362.

18. Madhav, M. R., Gurung, N., and Iwao, Y., 1998, "A Theoretical Model for the Pullout Response of Geosynthetic Reinforcement," *Geosynthetics International*, Vol. 5, No. 4, pp. 399-427.

19. Perkins, S. W. and Cuelho, E. V., 1999, "Soil-Geosynthetic Interface Strength and Stiffness Relationships from Pullout Tests," *Geosynthetics International*, Vol. 6, No. 5, pp. 321-346.

20. Negussey, D., and Jahanandish, M., 1993, "Comparison of Some Engineering Properties of Expanded Polystyrene with Those of Soils," *Transportation Research Record 1418*, Transportation Research Board, National Research Council, Washington, DC, pp. 43-50.

21. WisDOT, 2003, *Facilities Development Manual*, State of Wisconsin, Department of Transportation.

22. Kim, W. H., 2003, *Behavior of Geosynthetic-reinforced Aggregate Platforms Over Soft Subgrades*. PhD Dissertation, University of Wisconsin-Madison, Madison, Wisconsin.

23. Chew, S. H., Wong, W. K., Ng, C. C., Tan, S. A., and Karunaratne, G. P., 2000, "Strain Gauging Geotextiles Using External Gauge Attachment Method," Grips, Clamps, Clamping Techniques, and Strain Measurement for Testing of Geosynthetics, *ASTM STP 1379*, P.E. Stevenson, Eds., ASTM, West Conshohocken, PA, pp. 97-110.

24. Hayden, S. A., Humphrey, D. N., Christopher, B. R., Henry, K. S., and Fetten, C. P., 1999, "Effectiveness of Geosynthetics for Roadway Construction in Cold Regions: Results of a Multi-Use Test Section," *Proceedings of Geosynthetics '99*, Vol. 2, Boston, MA, pp. 847-862.

25. Tanyu, B. F., Benson, C. H., Edil, T. B., and Kim, W. H., 2004, "Equivalency of Crushed Rock and Three Industrial By-products Used for Working Platforms During Pavement Construction," *Transportation Research Record*, Paper No. 04-3105, Transportation Research Board, Washington, DC, (in press).

26. Giroud, J. P. and Han, J., 2004b, "Design Method for Geogrid-Reinforced Unpaved Roads. II. Development of Design Method," *Journal of Geotechnical Engineering Division*, ASCE, Vol. 130, No. 8, pp. 775-786.

LIST OF TABLES

Table 1. Properties of Grade 2 Gravel and Breaker Run Stone

Table 2. Properties of Geosynthetics.

Table 3. Thickness (m) of Working Platforms Required to Achieve Total Deflection (δ_t) of 12 mm, 25 mm, and 38 mm

LIST OF FIGURES

Fig. 1. Particle-size distributions of Grade 2 gravel and breaker run stone.

Fig. 2. Force-elongation curves from wide-width tensile tests on the geosynthetics: (a) machine direction and (b) cross-machine direction.

Fig. 3. Pull-out force vs. displacement at various points along the geosynthetic: (a) geogrid, (b) woven geotextile, (c) non-woven geotextile, and (d) drainage geocomposite.

Fig. 4. Schematic of large-scale model experiment (LSME).

Fig. 5. Cumulative total deflection (δ_t) under the loading plate of the LSME as a function of number of load cycles for working platforms having thickness (h) of 0.30 m or 0.46 m. Geosynthetic-reinforced working platforms were constructed with Grade 2 gravel.

Fig. 6. Effect of layer thickness (a) and type of geosynthetic (b) on total deflection basins at 1000 load cycles.

Fig. 7. Effect of layer thickness (a) and type of geosynthetic (b) on gage strain and telltale movement at the edge of the loading plate as a function of number of load cycles

Fig. 8. Thickness ratio for each of the working platforms for total deflections (at 1000 cycles) of 12, 25, and 38 mm.

Fig. 9. Relationship between thickness ratio and interaction modulus for total deflections (at 1000 cycles) of 25 and 38 mm.

Table 1. Properties of Grade 2 Gravel and Breaker Run Stone

Material	Specific Gravity	Size Fractions[a] (%)				C_u	USCS Symbol	Maximum Dry Unit Weight[b] (kN/m^3)
		Cobbles	Gravel	Sand	Fines			
Grade 2 Gravel	2.65	0	45	47	8	67	SW	22.6
Breaker Run	NM[c]	23	49	25	3	116	GW	NM[c]

Notes: [a]Soil faction refers to the fraction of breaker run smaller than 75 mm (both breaker runs contained cobbles larger than 75 mm), [b]Compaction per ASTM D 698, [c]NM = not measured.

Table 2. Properties of Geosynthetics.

Geosynthetic Type	Test	Property	Test Method	Values[g] (XMD)
Geogrid [a]	Wide Width Tensile Test	Thickness	ASTM D 5199	NM[h]
		Mass per Unit Area	ASTM D 5261	253.1 g/m^2
		Aperture Size[e]	NA[f]	32 (45) mm
		Peak Tensile Strength	GRI-GG1	17.2 (16.0) kN/m
		Yield Point Elongation	GRI-GG1	20 (11) %
		Offset Tangent Modulus	ASTM D 4595	88.3 (115) kN/m
	Pull-out Test[i]	Max. Pullout Force	GRI-GG6	25 kN/m
		Max. Front Displacement		35.8 mm
		Interaction Modulus		699 kPa
Woven Geotextile [b]	Wide Width Tensile Test	Thickness	ASTM D 5199	0.7 mm
		Mass per Unit Area	ASTM D 5261	268.2 g/m^2
		Wide Width Tensile	ASTM D 4595	35.3 (42.3) kN/m
		Wide Width Elongation	ASTM D 4595	26 (19) %
		Offset Tangent Modulus	ASTM D 4595	148 (292) kN/m
	Pull-out Test[i]	Max. Pullout Force	GRI-GT6	22 kN/m
		Max. Front Displacement		65.1 mm
		Interaction Modulus		338 kPa
Non-woven Geotextile [c]	Wide Width Tensile Test	Thickness	ASTM D 5199	2.7 mm
		Mass per Unit Area	ASTM D 5261	315.6 g/m^2
		Wide Width Tensile	ASTM D 4595	14.5 (21.8) kN/m
		Wide Width Elongation	ASTM D 4595	72 (57) %
		Offset Tangent Modulus	ASTM D 4595	34.0 (36.8) kN/m
	Pull-out Test[i]	Max. Pullout Force	GRI-GT6	12 kN/m
		Max. Front Displacement		156.7 mm
		Interaction Modulus		77 kPa
Drainage Geocomposite [d]	Wide Width Tensile Test	Thickness	ASTM D 5199	12.7 mm
		Mass per Unit Area	ASTM D 5261	1701 g/m^2
		Tensile Strength	ASTM D 4595	50.9 (54.4) kN/m
		Tensile Elongation	ASTM D 4595	57 (34) %
		Offset Tangent Modulus	ASTM D 4595	675 (200) kN/m
	Pull-out Test[i]	Max. Pullout Force	GRI-GT6	24 kN/m
		Max. Front Displacement		72.0 mm
		Interaction Modulus		333 kPa

Notes: [a] Biaxial oriented polypropylene, [b]polypropylene slit-film, [c]polypropylene needle punched, [d]tri-planar polyethylene geonet with non-woven polypropylene geotextiles, [e]reported by manufacturer, [f]NA=no standard method available, [g]machine direction (XMD=cross-machine direction), [h]NM = not measured, [i]cross-machine direction only.

Table 3. Thickness (m) of Working Platforms Required to Achieve Total Deflection (δ_t) of 12 mm, 25 mm, and 38 mm

Geosynthetic Reinforcement	Required Thickness (m)		
	δ_t = 12 mm	δ_t = 25 mm	δ_t = 38 mm
None (Breaker Run stone)	0.63	0.36	0.27
None (Grade 2 gravel)	0.69	0.41	0.31
Geogrid	0.42	0.28	0.22
Woven Geotextile	0.45	0.31	0.25
Nonwoven Geotextile	0.51	0.35	0.27
Drainage Geocomposite	0.53	0.33	0.25

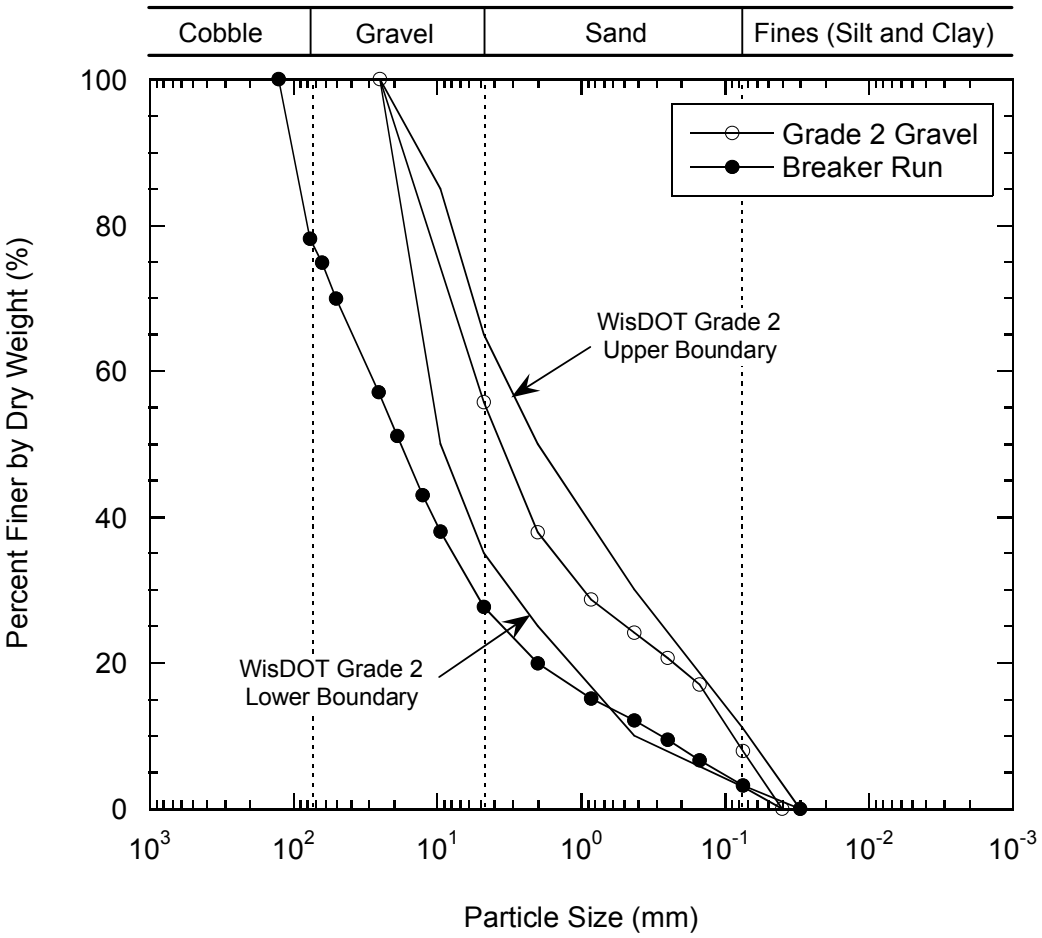

Fig. 1. Particle-size distributions of Grade 2 gravel and breaker run stone.

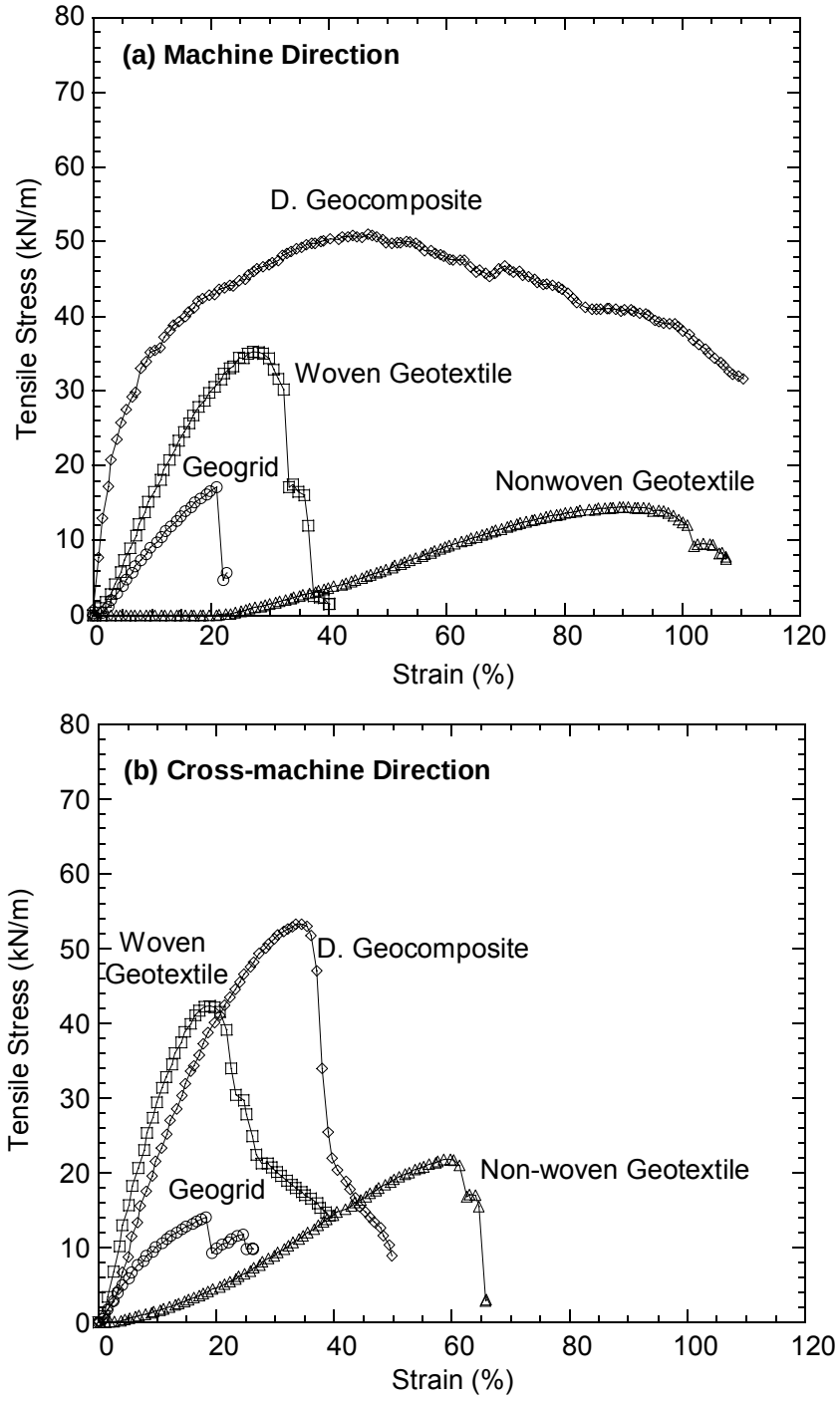

Fig. 2. Force-elongation curves from wide-width tensile tests on the geosynthetics: (a) machine direction and (b) cross-machine direction.

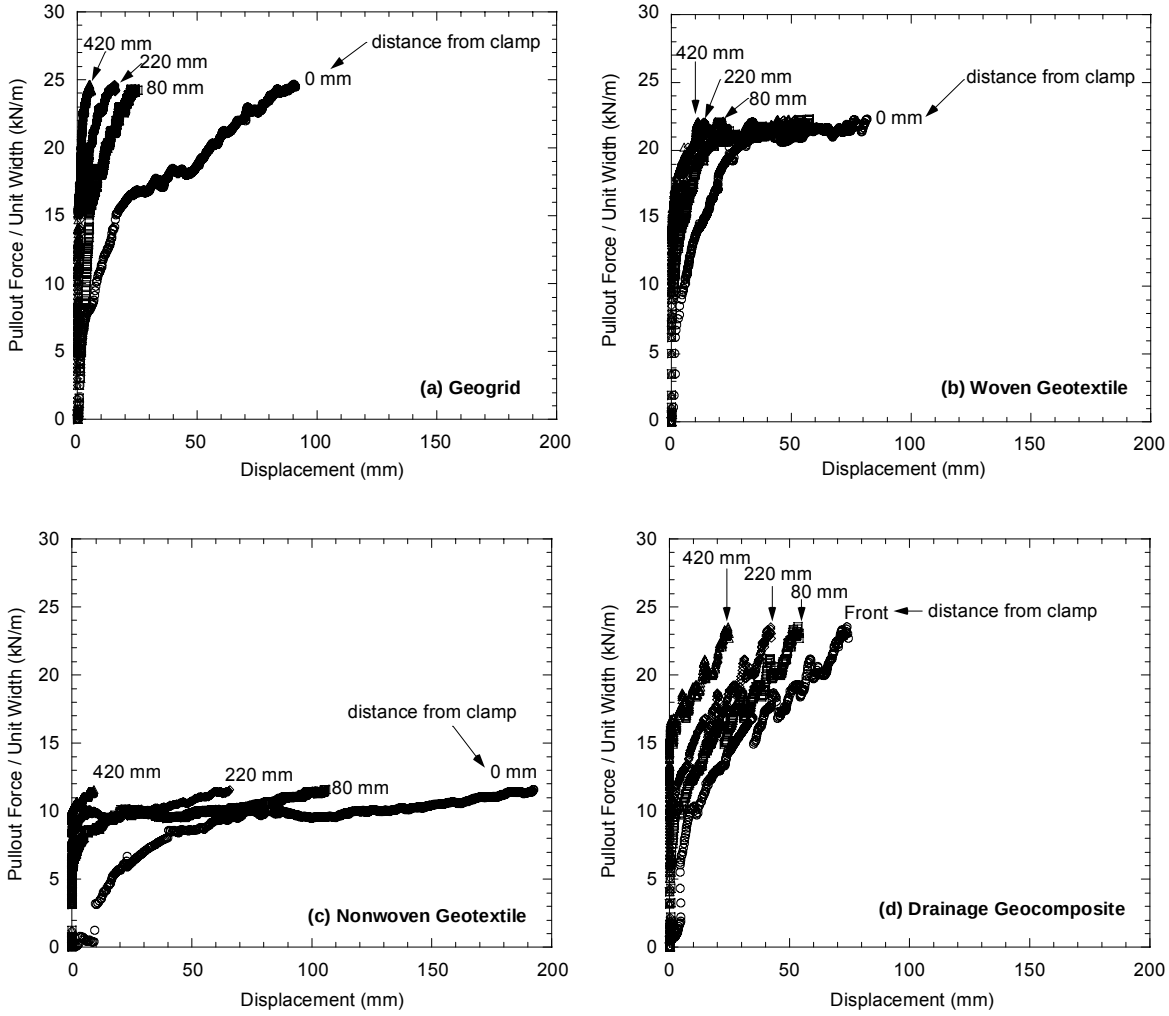

Fig. 3. Pull-out force vs. displacement at various points along the geosynthetic: (a) geogrid, (b) woven geotextile, (c) non-woven geotextile, and (d) drainage geocomposite.

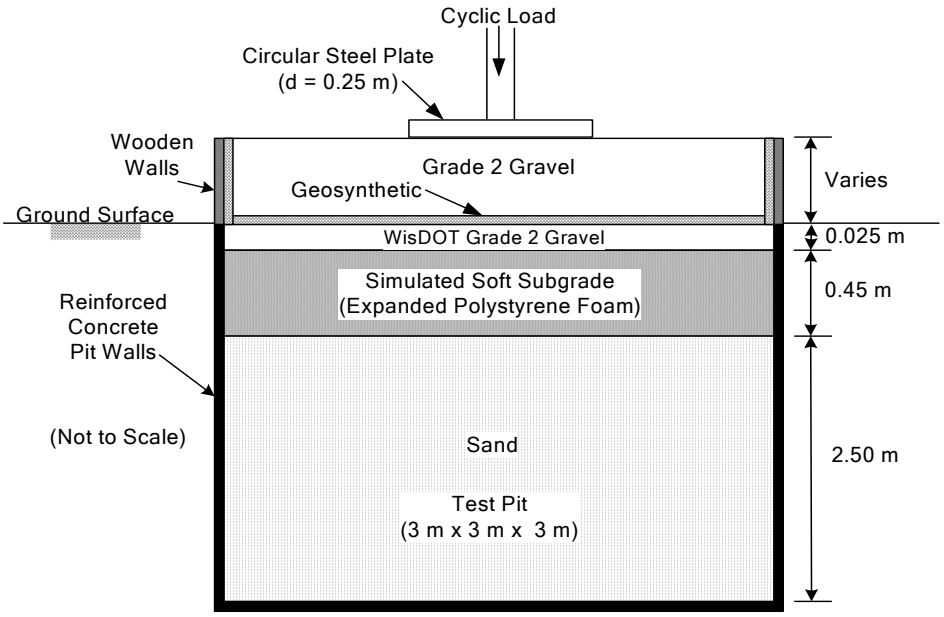

Fig. 4. Schematic of large-scale model experiment (LSME).

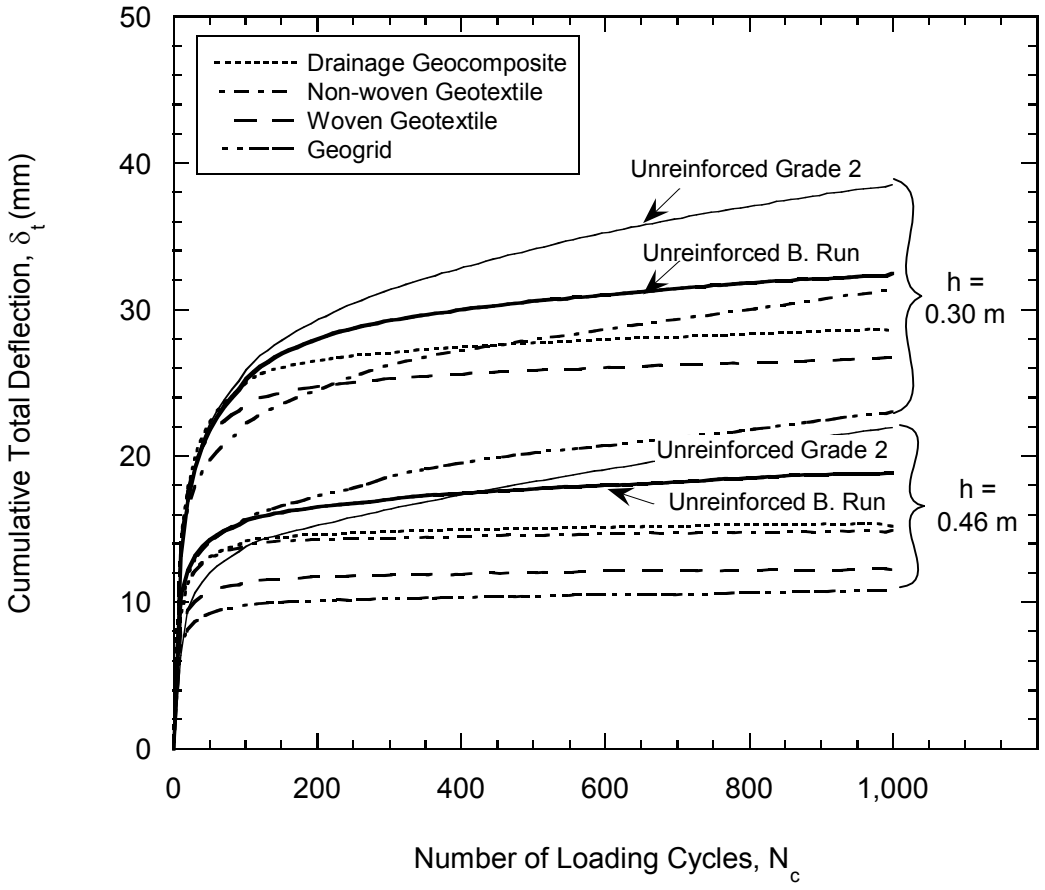

Fig. 5. Cumulative total deflection (δ_t) under the loading plate of the LSME as a function of number of load cycles for working platforms having thickness (h) of 0.30 m or 0.46 m. Geosynthetic-reinforced working platforms were constructed with Grade 2 gravel.

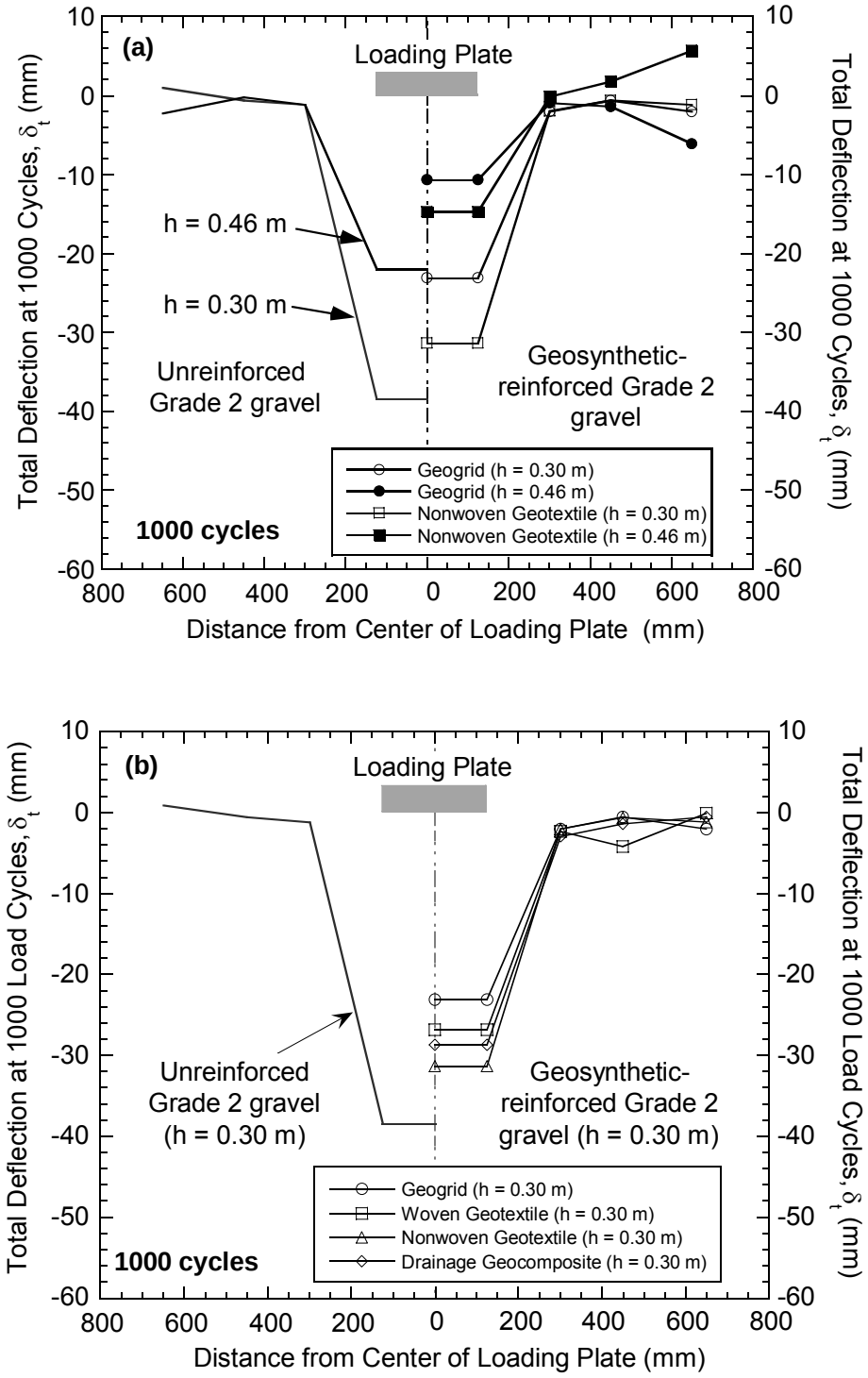

Fig. 6. Effect of layer thickness (a) and type of geosynthetic (b) on total deflection basins at 1000 load cycles.

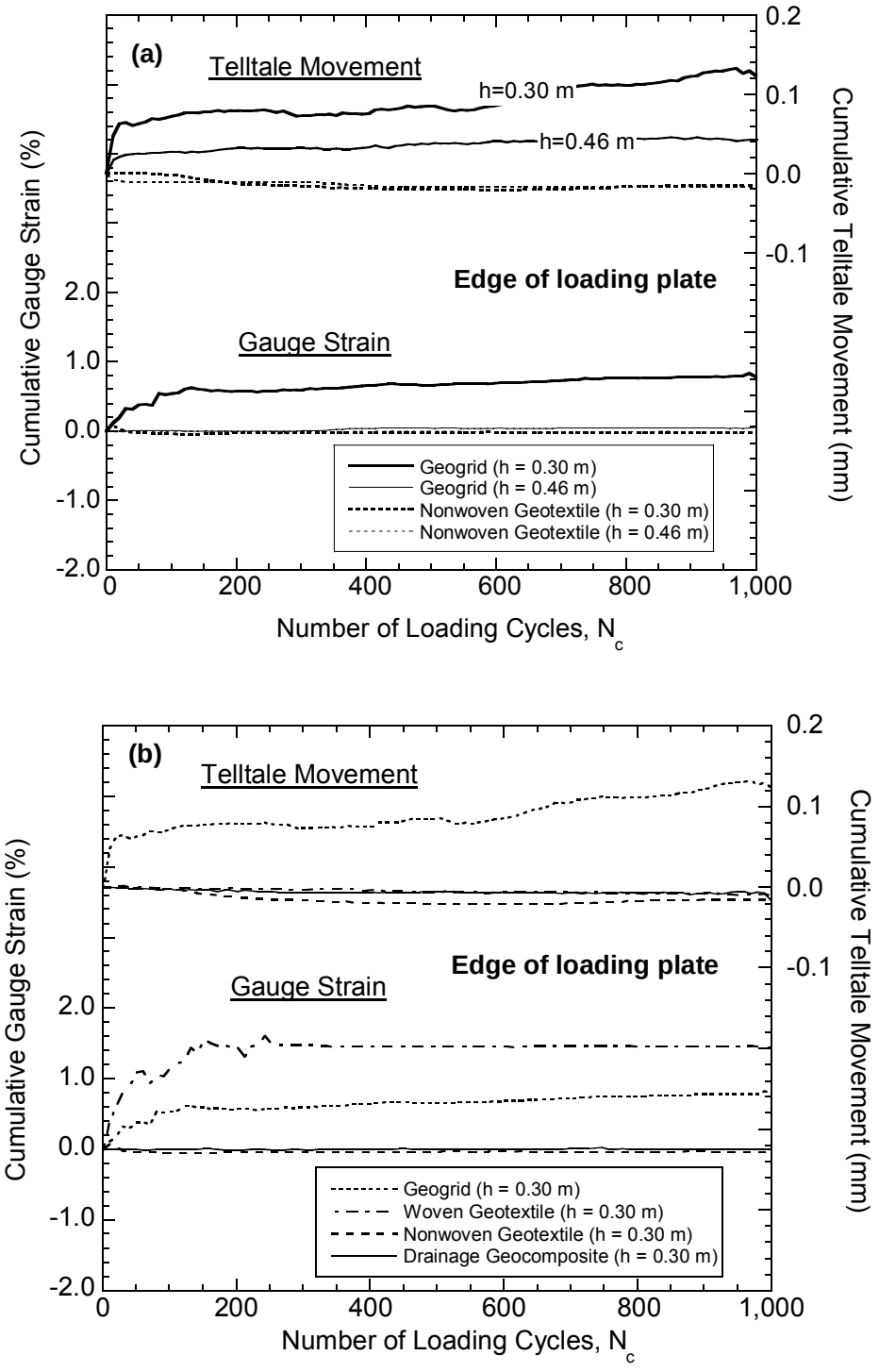

Fig. 7. Effect of layer thickness (a) and type of geosynthetic (b) on gage strain and telltale movement at the edge of the loading plate as a function of number of load cycles

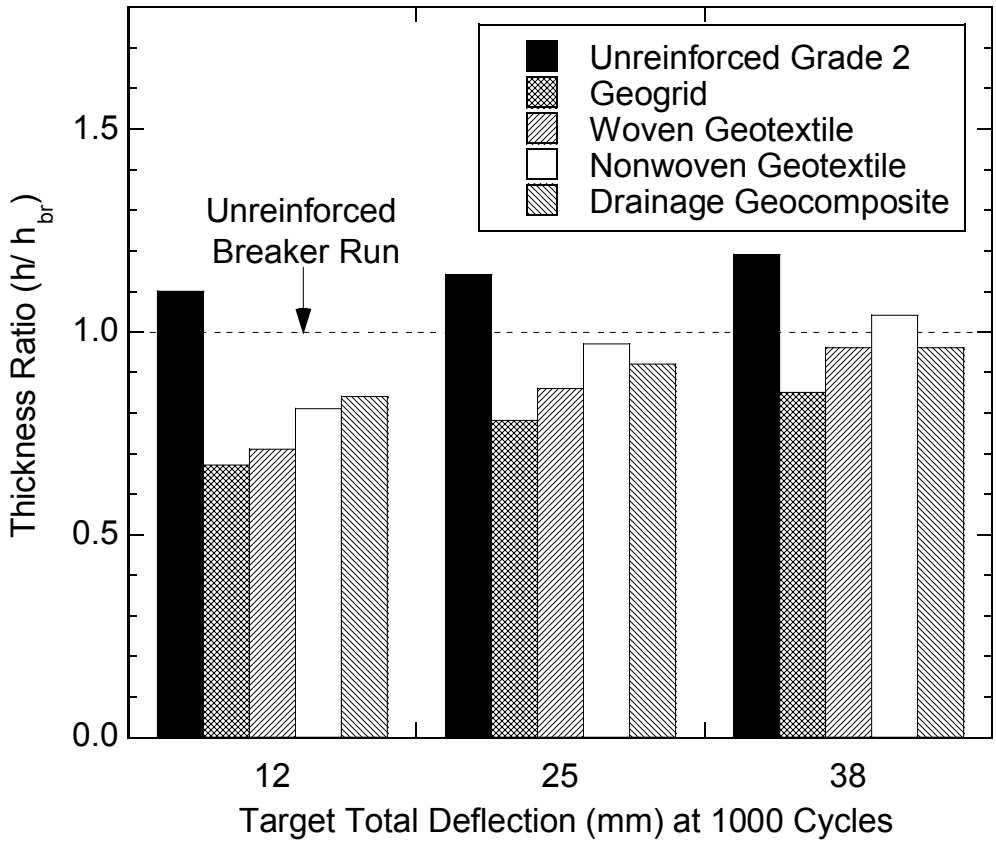

Fig. 8. Thickness ratio for each of the working platforms for total deflections (at 1000 cycles) of 12, 25, and 38 mm.

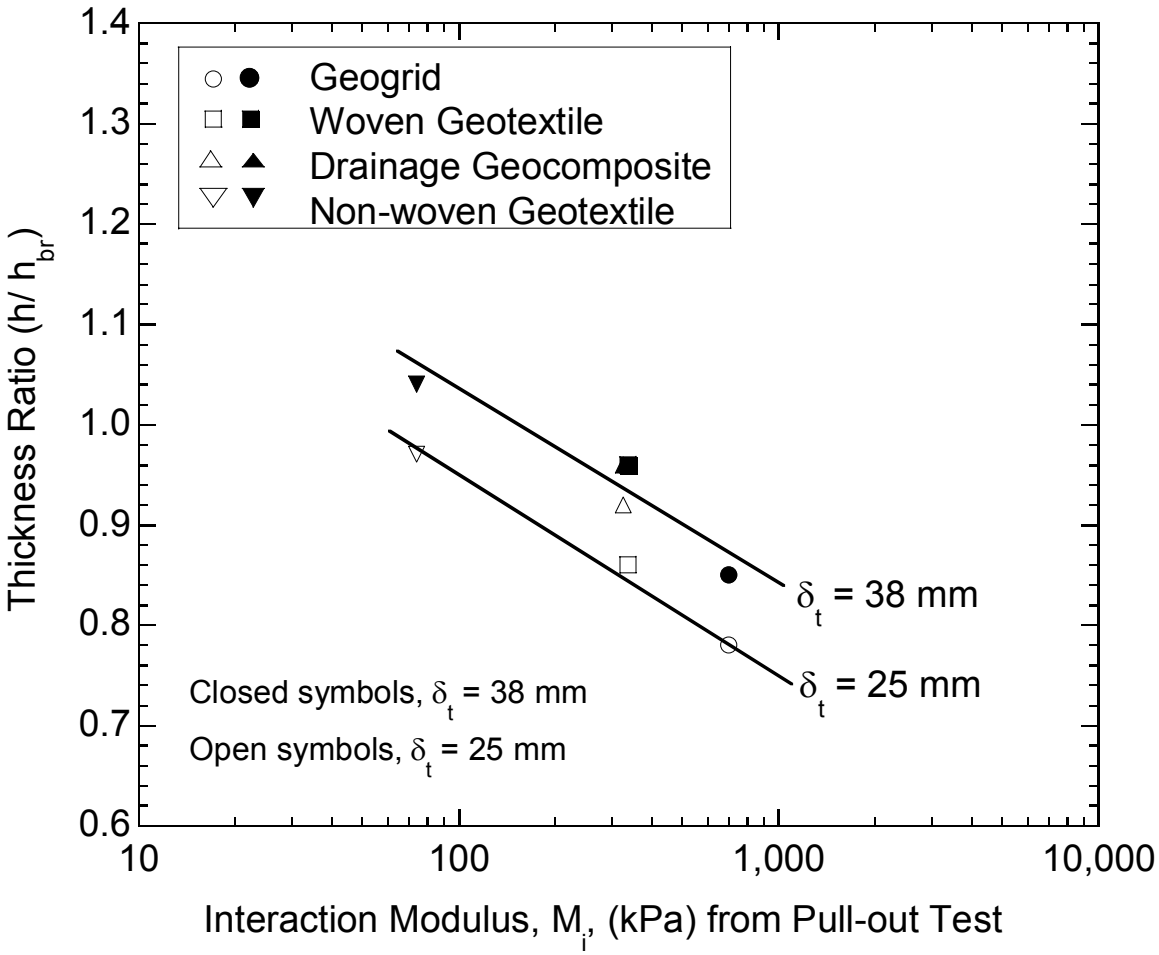

Fig. 9. Relationship between thickness ratio and interaction modulus for total deflections (at 1000 cycles) of 25 and 38 mm.